THE POLE CONDITION AS TRANSPARENT BOUNDARY CONDITION FOR RESONANCE PROBLEMS: DETECTION OF SPURIOUS SOLUTIONS*

B. KETTNER †

Abstract. When simulating isolated resonators, the application of transparent boundary conditions causes the approximated spectrum to be polluted with spurious solutions. Distinguishing these artificial solutions from solutions with a physical meaning is often difficult and requires a priori knowledge of the spectrum or the expected field distribution of resonant states. We present an implementation of the pole condition that distinguishes between incoming and outgoing waves by the location of the poles of their Laplace transform as transparent boundary condition. This implementation depends on one tuning parameter. We will use the sensitivity of the computed solutions to perturbations of this parameter as a means to identify spurious solutions. To obtain global statements, we will combine this technique with a convergence monitor for the boundary condition.

Key words. resonance problems, transparent boundary condition, pole condition, Helmholtz equation, spurious solutions

AMS subject classifications. 35Q60, 35J05, 35B34, 78M10, 15A18

1. Introduction. The problem of spurious solutions, that is unwanted solutions that have no physical meaning, has always accompanied the numerical approximation of resonance problems [16, 2, 3]. For closed resonators, it was overcome by Nédélecs introduction of edge elements [13], however though these special elements solved the problem from a practical point of view, the formal reason for their success was only given much later [4]. When turning from closed resonators with a perfectly conducting boundary towards open resonators, a new type of spurious solutions is introduced. These spurious solutions are caused by the application of transparent boundary conditions. Typically their detection requires a priori knowledge of the mode structure or of the field distribution of resonant states, which for complex resonator structures can not be taken for granted. We will introduce a method for the detection of the spurious solutions caused by transparent boundary conditions. We will use the Hardy space infinite element implementation [14, 12, 8] of the pole condition [18, 19] as transparent boundary condition and then use the sensitivity towards the perturbation of a parameter of the pole condition to identify spurious solutions of Helmholtz resonance problems.

This paper is structured as follows: first we will introduce the pole condition and discuss our implementation. The second section is devoted to deriving a way of identifying the spurious solutions within a computed eigenvalue spectrum. Finally we will give some examples.

2. The Pole Condition. The pole condition defines outward radiating solutions by the location of the poles of their transform with respect to a generalized distance variable in the complex plane and was developed by F. Schmidt [18, 19]. It is equivalent to the PML [10] and its correspondence with the Sommerfeld radiation condition for homogeneous exterior domains was shown by Hohage et al. [9]. In their review paper [1] Antoine et al. discuss its relation with other concepts for transparent boundary conditions for the Schrödinger equation. Our approach implements the

*This work was performed within project D23 of the DFG research center MATHEON.

†Konrad-Zuse-Zentrum für Informationstechnik Berlin (ZIB), Takustrae 7, 14195 Berlin (kettner@zib.de).

Hardy Space Infinite Element approach [14, 12, 8]. It is based on a Galerkin method in the Hardy space $H^+(D)$ of the complex unit disk. As we will see later in this section, the approach chosen here does not change the structure of the underlying eigenvalue problem since it is linear in the resonance frequency ω^2. Therefore the eigenvalue problems that will occur in our implementation can be solved with standard sparse eigenvalue solvers.

2.1. The Pole Condition in 1D . We will now derive the condition that refer to as the pole condition. We will start off with a variational formulation of the one-dimensional Helmholtz equation on an unbounded domain. By dividing the domain into a bounded interior and an unbounded exterior and restricting the test functions to a suitable set, we will obtain a formulation that contains the Laplace transforms of the solutions in the exterior parts. We will then give a derivation of the condition on the poles of the Laplace transform in terms of Cauchy's integral formula and a representation of the resulting path integral by Riemann sums.

Our starting point is the resonance mode setting of the one-dimensional Helmholtz equation on a possibly unbounded domain $\Omega \subseteq \mathbb{R}$:

$$\partial_{xx} u(x) + n(x)^2 \omega^2 u(x) = 0 \text{ for } x \in \Omega. \tag{2.1}$$

Multiplying with a test function $v \in H^1_{\text{loc}}(\Omega)$, the space of functions that restricted to a compact subset $\Omega_F \subset \Omega$ are in $H^1(\Omega_F)$, we obtain a weak formulation

$$\int_\Omega \partial_{xx} u(x) v(x) + n(x)^2 \omega^2 u(x) v(x) dx = 0 \tag{2.2}$$

for all $v \in H^1_{\text{loc}}(\Omega)$. Splitting Ω into a bounded interior Ω_{int} and an unbounded exterior $\Omega_{\text{ext}} = \mathbb{R} \backslash \Omega_{\text{int}}$ yields a splitting of the integral and after integrating the exterior integral by parts we obtain

$$\begin{aligned} &\int_{\Omega_{\text{int}}} \partial_{xx} u(x) v(x) + n(x)^2 \omega^2 u(x) v(x) dx + \\ &\int_{\Omega_{\text{ext}}} -\partial_x u(x) \partial_x v(x) + n_{l,r}^2 \omega^2 u(x) v(x) dx + u'(x) v(x)|_{x \in \partial\Omega_{\text{ext}}}. \end{aligned} \tag{2.3}$$

Next we insert the special forms $\Omega_{\text{int}} = [x_l, x_r]$ and $\Omega_{\text{ext}} = (-\infty, x_l] \cup [x_r, \infty)$ in the one-dimensional case into Equation (2.3) and have

$$\begin{aligned} &\int_{x_l}^{x_r} -\partial_x u(x) \partial_x v(x) + n(x)^2 \omega^2 u(x) v(x) dx + \\ &\int_{x<x_l} -\partial_x u(x) \partial_x v(x) + n_l^2 \omega^2 u(x) v(x) dx + u'(x_l) v(x_l) + \\ &\int_{x>x_r} -\partial_x u(x) \partial_x v(x) + n_r^2 \omega^2 u(x) v(x) dx - u'(x_r) v(x_r) = 0 \qquad \forall v \in H^1_{\text{loc}}(\Omega). \end{aligned} \tag{2.4}$$

Since it is sufficient to test against all functions v in a dense subset of $H^1_{\text{loc}}(\Omega)$, we will restrict the set of test functions for the exterior part to:

$$v_l(x) = c e^{-s(x_l - x)} \text{ for } x < x_l, \Re(s) > 0, c \in \mathbb{C} \text{ and} \tag{2.5}$$

$$v_r(x) = c e^{-s(x - x_r)} \text{ for } x > x_r, \Re(s) > 0, c \in \mathbb{C}. \tag{2.6}$$

After a further restriction to those functions with $c = 1$ and a coordinate transform, Equation (2.4) reads:

$$\begin{aligned} 0 = &\int_{x_l}^{x_r} -\partial_x u(x)\partial_x v(x) + n(x)^2\omega^2 u(x)v(x)dx \\ &+ \int_{x>0} \partial_x u(-x+x_l)se^{-sx} + n_l^2\omega^2 u(-x+x_l)e^{-sx}dx + u'(x_l) \\ &+ \int_{x>0} \partial_x u(x+x_r)se^{-sx} + n_r^2\omega^2 u(x+x_r)e^{-sx}dx + u'(x_r). \end{aligned} \tag{2.7}$$

The last two integrals are the Laplace transform of the Helmholtz equation in the left and right exterior domains:

DEFINITION 2.1. *The Laplace transform $\mathcal{L}\{f(t)\}(s)$ of a function $f : \mathbb{R}^+ \to \mathbb{C}$ is*

$$\mathcal{L}\{f(t)\}(s) := \int_0^\infty e^{-st} f(t)dt.$$

So renaming the solution in the left and right hand side exterior domain $u_{\text{ext},l}(x)$ and $u_{\text{ext},r}(x)$ respectively, we can rewrite Equation (2.7) in terms of $\mathcal{L}\{\partial_x u_{\text{ext},l}\}$, $\mathcal{L}\{\partial_x u_{\text{ext},r}\}$, $\mathcal{L}\{u_{\text{ext},l}\}$ and $\mathcal{L}\{u_{\text{ext},r}\}$:

$$\begin{aligned} 0 = &\int_{x_l}^{x_r} -\partial_x u(x)\partial_x v(x) + n(x)^2\omega^2 u(x)v(x)dx \\ &+ s\mathcal{L}\{\partial_x u_{\text{ext},l}\}(s) + n_l^2\omega^2\mathcal{L}\{u_{\text{ext},l}\}(s) + u'(x_l) \\ &+ s\mathcal{L}\{\partial_x u_{\text{ext},r}\}(s) + n_r^2\omega^2\mathcal{L}\{u_{\text{ext},r}\}(s) + u'(x_r). \end{aligned} \tag{2.8}$$

A central result of the Laplace transform is the Laplace transform of $\partial_x u(x)$. It can be obtained by integration by parts and states that

$$\mathcal{L}\{\partial_x u\}(s) = s\mathcal{L}\{u\}(s) - u(0). \tag{2.9}$$

We can now rewrite Equation (2.8) using Equation (2.9):

$$0 = \int_{x_l}^{x_r} -\partial_x u(x)\partial_x v(x) + n(x)^2\omega^2 u(x)v(x)dx \tag{2.10a}$$

$$+ s^2\mathcal{L}\{u_{\text{ext},l}\}(s) - su_{\text{ext},l}(x_l) + n_l^2\omega^2\mathcal{L}\{u_{\text{ext},l}\}(s) + u'(x_l) \tag{2.10b}$$

$$+ s^2\mathcal{L}\{u_{\text{ext},r}\}(s) - su_{\text{ext},r}(x_r) + n_r^2\omega^2\mathcal{L}\{u_{\text{ext},r}\}(s) + u'(x_r). \tag{2.10c}$$

While equation (2.10a) is the variational formulation for the solution in Ω_{int}, Equations (2.10b) and (2.10c) are the Laplace transforms of the original Helmholtz equation in the two sub-domains of Ω_{ext}.

We will now construct transparent boundary conditions by imposing conditions on these Laplace transforms $\mathcal{L}\{u_{\text{ext},l,r}\}(s)$. For an arbitrary function $u(x)$, its Laplace transform $\mathcal{L}\{u\}(s)$ as a function of s has some singularities in the complex plane. By Cauchy's integral formula

$$\mathcal{L}\{u\}(s) = \frac{1}{2\pi i}\oint_\gamma \frac{\mathcal{L}\{u\}(\tau)}{\tau - s}d\tau, \tag{2.11}$$

where γ is a path enclosing the singularities of $\mathcal{L}\{u\}$. Now we insert the Riemann sum for the path integral in (2.11) with an arbitrary parametrization of γ:

$$\mathcal{L}\{u\}(s) = \lim_{N\to\infty} \sum_{j=1}^{N} \alpha_j(N, \mathcal{L}\{u\}(\tau_j)) \frac{1}{\tau_j - s}. \tag{2.12}$$

In Equation (2.12), $\alpha_j(N, \mathcal{L}\{u\}(\tau_j))$ can be seen as weights and the entire sum may thus be reinterpreted as superposition of $(\tau - s)^{-1}$. Transforming these summands back into the space domain, we get the correspondence $(\tau - s)^{-1} \leftrightarrow -\exp(\tau x)$. Depending on the location of τ in the complex plane $\mathbb{C}$, $-\exp(\tau x)$ is moving to the left/exponentially increasing or moving to the right/exponentially decreasing. So for each disjoint subset of Ω_{ext}, the complex plane can be divided into the two regions

$$\begin{aligned}\mathbb{C}_{in} &:= \{\tau \in \mathbb{C} : -\exp(\tau x) \text{ is incoming or not oscillating}\} \text{ and}\\ \mathbb{C}_{out} &:= \{\tau \in \mathbb{C} : -\exp(\tau x) \text{ is outward radiating}\}.\end{aligned}$$

This enables us to split the path γ from (2.11) into two paths $\gamma_{in} \subset \mathbb{C}_{in}$ and $\gamma_{out} \subset \mathbb{C}_{out}$ that each enclose all the singularities of $\mathcal{L}\{u\}(s)$ in the respective region. Equation (2.11) then decomposes as follows:

$$\mathcal{L}\{u\}(s) = \oint_{\gamma_{in}} \frac{\mathcal{L}\{u\}(\tau)}{\tau - s} d\tau + \oint_{\gamma_{out}} \frac{\mathcal{L}\{u\}(\tau)}{\tau - s} d\tau. \tag{2.13}$$

Requiring that u is outward radiating is equivalent to requiring that $\oint_{\gamma_{in}} \frac{\mathcal{L}\{u\}(\tau)}{\tau - s} d\tau$ is zero. This corresponds to the condition that $\mathcal{L}\{u\}(s)$ is analytic in $\mathbb{C}_{in}$. The splitting into $\mathbb{C}_{in}$ and $\mathbb{C}_{out}$ is possible whenever it is possible to distinguish between incoming and outgoing solutions, that is when the problem is not degenerated. We are now in the position to summarize the method in the following definition:

DEFINITION 2.2. *A function $u \in H^1(\Omega)$ is said to obey the pole condition if the complex continuation of its Laplace transform $\mathcal{L}\{u\}(s)$ is analytic in $\mathbb{C}_{in}$.*

Now we will apply this to the one-dimensional Helmholtz resonance problem. Suppose that u_{int} is given inside $\Omega_{\text{int}} = [x_l, x_r]$. Since the following considerations are the same for the left and right exterior domains, we will take into account only the right hand component of the exterior domain. Then the equation for $\mathcal{L}\{u_{\text{ext},r}\}(s)$ derived from Equation (2.10c) is

$$\begin{aligned}0 &= s^2 \mathcal{L}\{u_{\text{ext},r}\}(s) - s u_{\text{ext},r}(x_r) + n_r^2 \omega^2 \mathcal{L}\{u_{\text{ext},r}\}(s) + u'(x_r)\\ \Leftrightarrow \mathcal{L}\{u_{\text{ext},r}\} &= (s^2 + n_r^2\omega^2)^{-1}(s u_{\text{ext},r} + u'(x_r)).\end{aligned}$$

For fixed ω, $(s^2 + n_r^2\omega^2)$ has two roots $s_{+/-} = \pm i\sqrt{n_r^2\omega^2}$, so we can obtain a partial fraction decomposition of $\mathcal{L}\{u_{\text{ext},r}\}$:

$$\begin{aligned}\mathcal{L}\{u_{\text{ext},r}\}(s) =& (s + s_+)^{-1} \frac{1}{2} \left(u_{\text{ext},r}(x_r) + u'(x_r)\right) +\\ & (s + s_-)^{-1} \frac{1}{2} \left(u_{\text{ext},r}(x_r) + u'(x_r)\right).\end{aligned} \tag{2.14}$$

Transforming the summands in Equation (2.14) back to the space domain, they correspond to

$$e^{-s_+ x}((u_{\text{ext},r}(x_r) + u'(x_r))/2) \text{ and } e^{-s_- x}((u_{\text{ext},r}(x_r) + u'(x_r))/2).$$

Depending on the location of $s_{+/-}$ in the complex plane, they are incoming, exponentially increasing, outgoing or exponentially decreasing. For the left boundary we can obtain a similar splitting by the same arguments.

2.2. Implementation. We will now derive an implementation of the pole condition that fits into the finite element context. The outline of what follows next is:

1. Define a mapping $P_{s_0} := \mathbb{C}_{in} \to D$, obtain a mapping $H^-(P_{s_0}) \to H^+(D)$.
2. Reformulate the pole condition in terms of these function spaces.
3. Approximate a function in $H^+(D)$ with a power series to obtain a discrete formulation.
4. Choose a test-function for the exterior domain such that the previous formulation can be embedded within a finite element context.
5. Derive the local element matrices this yields for each component of the exterior domain.

For connecting the half space $P_{s_0} := \{z \in \mathbb{C} : \Re(z/s_0) \leq 0\}$ below the line connecting 0 and is_0 with the unit disc, we use the Möbius transform and its inverse, see Fig. 2.1:

$$\mathcal{M}_{s_0}(s) = \widetilde{s} := \frac{s + s_0}{s - s_0} \quad \text{and } \mathcal{M}_{s_0}^{-1} : \widetilde{s} \to s = s_0 \frac{\widetilde{s} + 1}{\widetilde{s} - 1}. \tag{2.15}$$

The complex parameter s_0 determines the position of the half-space and acts as a tuning parameter. It will be used to identify the spurious modes of the resonance problem at a later point. Since we require $\mathcal{L}\{u\}(s)$ to be analytic in $\mathbb{C}_{in}$, we can use the property that an analytic function can be expanded into a power series that converges inside some ball to obtain a formulation of the pole condition that can be implemented. $\mathcal{M}_{s_0}$ maps the infinite point to 1 and s_0 to zero, thus an approximation of $\mathcal{L}\{u_{\text{ext}}\} \circ \mathcal{M}_{s_0}$ by an power series expansion will be best near s_0. So choosing s_0 in the region where one expects the resonances of interest to be located is typically a good choice.

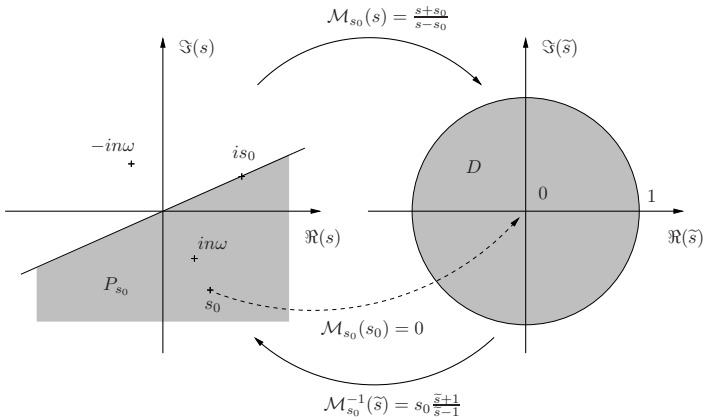

FIG. 2.1. *The Möbius transform $\mathcal{M}_{s_0}$ and its inverse.*

In order to be able to give a formal definition of the pole condition in the setting that is fit for implementation, we will have to give some definitions of the function spaces on P_{s_0} and D.

DEFINITION 2.3. *As before let $P_{s_0} := \{z \in \mathbb{C} : \Re(z/s_0) \leq 0\}$ be the half space below the line connecting 0 and is_0. The Hardy Space $H^-(P_{s_0})$ is the space of all*

functions u that are holomorphic in P_{s_0} such that

$$\int_{\mathbb{R}} |u(s_0 x - s_0 i\epsilon)| dx$$

is uniformly bounded for $\epsilon > 0$.
Let $D = \{z \in \mathbb{C} : |z| < 1\}$ be the open unit disc in $\mathbb{C}$. The Hardy Space $H^+(D)$ is the space of all functions u that are holomorphic in D such that

$$\int_0^{2\pi} |u(re^{it})|^2 dt$$

is uniformly bounded for $r \in [0, 1]$.

Since u in both parts of Definition 2.3 are uniformly bounded, there exist L^2 functions on the boundary of the domains that are uniquely defined by u and in turn uniquely define u. This allows us to identify functions in the Hardy Spaces $H^-(P_{s_0})$ and $H^+(D)$ with their boundary functions in $L^2(P_{s_0})$ or $L^2(S^1)$ respectively.

The Möbius transform does not only connect P_{s_0} and D, it also forms a connection between the function spaces $H^-(P_{s_0})$ and $H^+(D)$:

$$f \in H^-(P_{s_0}) \to H^+(D) \ni (\mathcal{M}_{s_0} f)(\widetilde{s}) := f\left(\mathcal{M}_{s_0}^{-1}(\widetilde{s})\right) \frac{1}{\widetilde{s} - 1}. \tag{2.16}$$

We can now reformulate the pole condition from Definition 2.2 in terms of the function spaces from Definition 2.3:

Definition 2.4. *Let $s_0 \in \mathbb{C}$ with $\Re(s_0) > 0$. Then a solution to Equation (2.1) is said to obey the pole condition and is called outgoing if $\mathcal{M}_{s_0}\mathcal{L}\{u_{ext}\}(\widetilde{s})$, the Möbius transform $\mathcal{M}_{s_0}$ of the holomorphic extension of the Laplace transform of the exterior part, lies in $H^+(D)$.*

We can use Equation (2.16) to define $\mathcal{L}_D$, the Laplace transform on the unit disc D. Since this can be done in the same way for both $u_{\text{ext},l}$ and $u_{\text{ext},r}$ we will give the formulation only for the right exterior domain.

$$\mathcal{L}_D\{u_{\text{ext},r}\}(\widetilde{s}) := \mathcal{L}\{u_{\text{ext},r}\}\left(\mathcal{M}_{s_0}^{-1}(\widetilde{s})\right) \frac{1}{\widetilde{s} - 1}. \tag{2.17}$$

Since we require the Laplace transform to be analytic in the unit disc, it can be expanded into a power series, $\mathcal{L}_D\{u_{\text{ext}}\}(\widetilde{s}) = \sum_{k=0}^{\infty} a_k \widetilde{s}^k$. Hence

$$\mathcal{L}\{u_{\text{ext},r}\}\left(\mathcal{M}_{s_0}^{-1}(\widetilde{s})\right) = (\widetilde{s} - 1) \sum_{k=0}^{\infty} a_k \widetilde{s}^k. \tag{2.18}$$

We will now describe the implementation of a transparent boundary condition based on the pole condition within a finite element context for the one-dimensional problem in some detail. The discretization for higher space dimensions is typically done via Cartesian products and will be detailed in the next section.

As before we will use ansatz functions that directly yield the Laplace transform in the exterior domain Ω_{ext}. These ansatz functions are called "boundary exp-elements" and consist of the standard interior element coupled with a complex exponential function that will result in a formulation of the Laplace transform in the exterior. Such an element is sketched in Fig. 2.2 for a linear discretization in the interior.

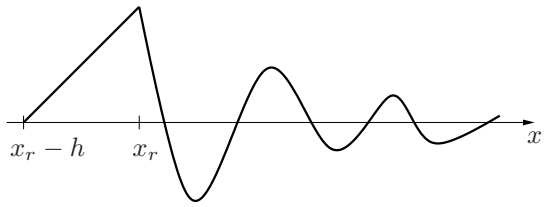

FIG. 2.2. *Exp-element for the right hand side boundary with first order discretization in the interior.*

The boundary exp-element test function for polynomial degree $p = 1$ in the interior at the right artificial boundary x_r is given by

$$\psi_s^{(r)}(x) = \begin{cases} e^{-s(x-x_r)} : x \geq x_r, \\ \frac{x-(x_r-h)}{h} : x_r - h \leq x \leq x_r. \end{cases} \tag{2.19}$$

The exp-element $\psi_s^{(r)}(x)$ is not one function but a family of functions parametrized by $s \in \mathbb{C}^+$. They are globally continuous by definition and their support is infinite: $\text{supp}\left(\psi_x^{(r)}\right) = [x_r - h, \infty)$. By using $\psi_s(x)$ as test function in the variational formulation (2.2), we obtain

$$0 = \int_{\mathbb{R}} -\partial_{xx} u_{\text{int}}(x)\psi_s(x) + \omega^2 n(x)^2 u_{\text{int}}(x)\psi_s(x)dx$$

Due to the definition of $\psi_s(x)$ and assuming that $n(x) \equiv n_i$ for $x \in [x_r - h, x_r]$ and $n(x) \equiv n_r$ for $x > x_r$, after integration by parts we obtain:

$$\begin{aligned} 0 = &- \int_{x_r-h}^{x_r} \partial_x u_{\text{int}}(x)\frac{1}{h}dx + \omega^2 n_i^2 \int_{x_r-h}^{x_r} u_{\text{int}}(x)\frac{x-(x_r-h)}{h}dx \\ &+ s\left(s\mathcal{L}\{u_{\text{ext},r}\}(s) - u_{\text{ext},r}(x_r)\right) + \omega^2 n_r^2 \mathcal{L}\{u_{\text{ext},r}\}(s). \end{aligned} \tag{2.20}$$

The boundary Neumann terms occurring due to the integration by parts are here given in weak form in the first integrals. We have now obtained $\mathcal{L}\{u_{\text{ext},r}\}$ but this does not yield a discrete formulation since we lack a convenient orthonormal basis for $H^-(P_{s_0})$. To remedy this deficit, we will transform Equation (2.20) to $H^+(D)$ by applying (2.17) and inserting $\widetilde{s}$ as defined in Equation (2.15):

$$\begin{aligned} 0 = &- \int_{x_r-h}^{x_r} \partial_x u_{\text{int}}(x)\frac{1}{h}dx + \omega^2 n_i^2 \int_{x_r-h}^{x_r} u_{\text{int}}(x)\frac{x-(x_r-h)}{h}dx \\ &+ s_0\frac{\widetilde{s}+1}{\widetilde{s}-1}\left(s_0\frac{\widetilde{s}+1}{\widetilde{s}-1}(\widetilde{s}-1)\mathcal{L}_D\{u_{\text{ext},r}\}(\widetilde{s}) - u_{\text{ext},r}(x_r)\right) \\ &+ \omega^2 n_r^2(\widetilde{s}-1)\mathcal{L}_D\{u_{\text{ext},r}\}(\widetilde{s}). \end{aligned} \tag{2.21}$$

The next step is to insert a series expansion for $\mathcal{L}_D\{u_{\text{ext},r}\}(\widetilde{s})$. However, for ease of implementation we will not use the direct power series approximation from Equation (2.18) but reformulate it. To obtain an easy formulation for the coupling of the transformed exterior to the interior problem, we use Equation (2.14) to reformulate:

$$\begin{aligned} \mathcal{L}\{u_{\text{ext},l,r}\}(s) &= \frac{u_{\text{int}}(x_{l,r})}{s - in_{l,r}\omega} \\ \xrightarrow{\mathcal{M}_{s_0}} \mathcal{L}_D\{u_{\text{ext},l,r}\}(\widetilde{s}) &= \frac{u_{\text{int}}(x_{l,r})}{s_0(\widetilde{s}+1) - in_{l,r}\omega(\widetilde{s}-1)}. \end{aligned} \tag{2.22}$$

If we would attempt to do a power series approximation of Equation (2.22), the boundary degree of freedom $u_{\text{int}}(x_{l,r})$ would couple with each degree of freedom in the exterior. In order to obtain a local coupling, we note that $\mathcal{L}_D\{u_{\text{ext},l,r}\}(1) = u_{\text{int}}(x_{l,r})/2s_0$. To take advantage of this fact, we now decompose

$$\mathcal{L}_D\{u_{\text{ext},l,r}\}(\widetilde{s}) = \frac{1}{2s_0}\left(u_{\text{int}}(x_{l,r}) + (\widetilde{s}-1)\frac{2s_0\mathcal{L}_D\{u_{\text{ext}}\}(\widetilde{s}) - u_{\text{int}}(x_{l,r})}{\widetilde{s}-1}\right). \tag{2.23}$$

Inserting the series representation (2.18) and rescaling its coefficients we have

$$\mathcal{L}_D\{u_{\text{ext},l,r}\}(\widetilde{s}) = \frac{u_{\text{int}}(x_{l,r})}{2s_0} + (\widetilde{s}-1)\frac{1}{2s_0}\sum_{k=0}^{\infty}\widetilde{a}_k\widetilde{s}^k. \tag{2.24}$$

Inserting (2.24) into Equation (2.21), we get for the right hand side boundary

$$0 = -\int_{x_r-h}^{x_r}\partial_x u_{\text{int}}(x)\frac{1}{h}dx + \int_{x_r-h}^{x_r}u_{\text{int}}(x)\frac{x-(x_r-h)}{h}dx \tag{2.25a}$$

$$+ u_{\text{int}}(x_r)\frac{s_0}{2}(\widetilde{s}+1) + \frac{s_0}{2}(\widetilde{s}+1)^2\sum_{k=0}^{\infty}\widetilde{a}_k\widetilde{s}^k \tag{2.25b}$$

$$+ \omega^2 n_r^2\left(u_{\text{int}}(x_r)\frac{1}{2s_0}(\widetilde{s}-1) + \frac{1}{2s_0}(\widetilde{s}-1)^2\sum_{k=0}^{\infty}\widetilde{a}_k\widetilde{s}^k\right). \tag{2.25c}$$

In order to obtain the local element matrix for the exp-element, we sort (2.25a)-(2.25c) by powers of $\widetilde{s}$, compare coefficients and truncate by setting $a_k = 0$ for $k \geq L$:

$$\widetilde{s}^0:\ 0 = -\int_{x_r-h}^{x_r}\partial_x u_{\text{int}}(x)dx + \omega^2 n_i^2\int_{x_r-h}^{x_r}u_{\text{int}}(x)\frac{x-(x_r-h)}{h}dx$$
$$+ \frac{s_0}{2}\left(u_{\text{int}}(x_r) + \widetilde{a}_0\right) - \omega^2 n_r^2\frac{1}{2s_0}\left(u_{\text{int}}(x_r) - \widetilde{a}_0\right) \tag{2.26a}$$

$$\widetilde{s}^1:\ 0 = \frac{s_0}{2}\left(u_{\text{int}}(x_r) + 2\widetilde{a}_0 + \widetilde{a}_1\right) - \omega^2 n_r^2\frac{1}{2s_0}\left(-u_{\text{int}}(x_r) + 2\widetilde{a}_0 - \widetilde{a}_1\right) \tag{2.26b}$$

$$\widetilde{s}^k:\ 0 = \frac{s_0}{2}\left(\widetilde{a}_{k-2} + 2\widetilde{a}_{k-1} + \widetilde{a}_k\right) - \omega^2 n_r^2\frac{1}{2s_0}\left(-\widetilde{a}_{k-2} + 2\widetilde{a}_{k-1} - \widetilde{a}_k\right)$$
$$2 \leq k \leq L. \tag{2.26c}$$

Collecting these degrees of freedom, we get the following local element $L \times L$-matrices for the exterior part of the infinite exp-element:

$$A_{\text{ext}}^{\text{loc}} = s_0\frac{1}{2}\begin{pmatrix} 1 & 1 & 0 & \cdots & & \\ 1 & 2 & 1 & 0 & \cdots & \\ 0 & 1 & 2 & 1 & 0 & \cdots \\ & & \ddots & \ddots & \ddots & \end{pmatrix} \tag{2.27}$$

and

$$B_{\text{ext}}^{\text{loc}} = n_{l,r}^2\frac{1}{2s_0}\begin{pmatrix} 1 & -1 & 0 & \cdots & & \\ -1 & 2 & -1 & 0 & \cdots & \\ 0 & -1 & 2 & -1 & 0 & \cdots \\ & & \ddots & \ddots & \ddots & \end{pmatrix}. \tag{2.28}$$

The first degree of freedom in these local element matrices is $u_{\text{int}}(x_{l,r})$ that is common to the interior and the exterior solution and thus provides the coupling. The integral terms occurring for $\widetilde{s}^0$ are the weak formulation of the Neumann data and can be assembled together with the interior degrees of freedom. Discretization of Ω_{int} with normal finite elements yields a sparse eigenvalue problem with mass matrix A_{int}, system matrix B_{int} and vector of unknowns $\mathbf{u}_{\text{int}}$:

$$\left(A_{\text{int}} - \omega^2 B_{\text{int}}\right) \mathbf{u}_{\text{int}} = 0. \tag{2.29}$$

Combining the degrees of freedom $\widetilde{a}_k$ in the exterior with the degrees of freedom $\mathbf{u}_{\text{int}}$ in the interior and collecting them into one vector of unknowns $\mathbf{u}$, we arrive at a generalized sparse eigenvalue problem $(A-\omega^2 B)\mathbf{u} = 0$. Using linear finite elements in the interior and first order exp-elements in the exterior, A and B have the structure as sketched in Fig. 2.3.

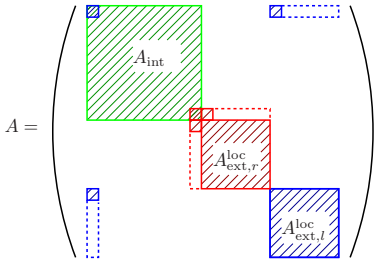

FIG. 2.3. *Structure for sparse matrix A for a one-dimensional Helmholtz resonance problem. B has the same structure with coupling in only one interior degree of freedom.*

In order to insert the exterior degrees of freedom into the global matrices A and B, we need a mapping P that maps the local degrees of freedom of a component of the exterior domain to the global degrees of freedom. If we call the mapping for the left hand exterior domain degrees of freedom P_l and the mapping for the right hand exterior domain degrees of freedom P_r, the $N \times N$ matrices $P_l^\top A^{\text{loc}}_{\text{ext},l} P_l$, $P_r^\top A^{\text{loc}}_{\text{ext},r} P_r$, $P_l^\top B^{\text{loc}}_{\text{ext},l} P_l$ and $P_r^\top B^{\text{loc}}_{\text{ext},r} P_r$ are the contributions of the left and right exterior domain to the global system matrices A and B, together they give the exterior parts A_{ext} and B_{ext} of A and B:

$$A_{\text{ext}} = (P_l^\top A^{\text{loc}}_{\text{ext},l} P_l + P_r^\top A^{\text{loc}}_{\text{ext},r} P_r) \text{ and} \tag{2.30}$$

$$B_{\text{ext}} = (n_l^2 P_l^\top B^{\text{loc}}_{\text{ext},l} P_l + n_r^2 P_r^\top A^{\text{loc}}_{\text{ext},r} P_r) \tag{2.31}$$

2.3. Alternative Approach: Variational Formulation.

$$\mathbf{T}^{(-)} \begin{pmatrix} f_0 \\ F \end{pmatrix} := \frac{1}{2}(f_0 + (\widetilde{s} - 1)F(\widetilde{s})) \tag{2.32}$$

for $(f_0, F)^\top \in \mathbb{C} \times H^+(D)$ where f_0 is the boundary degree of freedom. Next we will make use of the identity

$$\int_0^\infty f(\tau) g(\tau) d\tau = \frac{-s_0}{\pi} \int_{S^1} \mathcal{L}_D\{f\}(\overline{z}) \mathcal{L}_D\{g\}(z) dz. \tag{2.33}$$

A full formal proof of this equality uses properties of the Fourier transform and can be found at [12, Lemma 5.3] and [8, Lemma A.1]. Substituting $A(F, G) :=$

$\frac{1}{2\pi}\int_{S^1} F(\overline{z})G(z)d|z|$ for $F, G \in H^+(D)$ for brevity, Equation (2.33) reads

$$\int_0^\infty f(\tau)g(\tau)d\tau = -2s_0 A(\mathcal{L}_D\{f\}, \mathcal{L}_D\{g\}). \tag{2.34}$$

This holds for u_{ext} and suitable test functions v_{ext} as well as for the derivatives u'_{ext} and v'_{ext}. In order to obtain simple formulas for the derivatives u'_{ext} and v'_{ext}, we again use the basic property of the Laplace transform

$$\mathcal{L}\{f'\}(s) = s\mathcal{L}\{f\}(s) - f_0. \tag{2.35}$$

By applying the Möbius transform to Equation (2.35), we have

$$\begin{aligned}
\mathcal{M}_{s_0}\mathcal{L}\{f'\}(\widetilde{s}) &= s_0\frac{\widetilde{s}+1}{\widetilde{s}-1}\mathcal{L}_D\{f\}(\widetilde{s}) - \frac{f_0}{\widetilde{s}-1} \\
&= \frac{1}{2}(f_0 + (\widetilde{s}+1)F(\widetilde{s}))\left(\text{with } F(\widetilde{s}) = \frac{2s_0\mathcal{L}_D\{f\}(\widetilde{s}) - f_0}{\widetilde{s}-1}\right) \\
&=: \mathbf{T}^{(+)}\begin{pmatrix} f_0 \\ F \end{pmatrix}
\end{aligned} \tag{2.36}$$

Now we are able to deduce from the variational formulation (2.2) and the identity (2.34) a variational formulation in $H^1(\Omega_{\text{int}}) \times H^+(D)$:

$$B\left(\begin{pmatrix} u_{\text{int}} \\ U \end{pmatrix}, \begin{pmatrix} v_{\text{int}} \\ V \end{pmatrix}\right) = 0 \tag{2.37}$$

with

$$\begin{aligned}
B\left(\begin{pmatrix} u_{\text{int}} \\ U \end{pmatrix}, \begin{pmatrix} v_{\text{int}} \\ V \end{pmatrix}\right) &:= \int_{\Omega_{\text{int}}} u'_{\text{int}}(x)v'_{\text{int}}(x) - n(x)^2\omega^2 u_{\text{int}}(x)v_{\text{int}}(x)dx \\
-2s_0 A\left(\mathbf{T}^{(+)}\begin{pmatrix} u_0 \\ U \end{pmatrix}, \mathbf{T}^{(+)}\begin{pmatrix} v_0 \\ V \end{pmatrix}\right) &- \frac{2n^2\omega^2}{s_0} A\left(\mathbf{T}^{(-)}\begin{pmatrix} u_0 \\ U \end{pmatrix}, \mathbf{T}^{(-)}\begin{pmatrix} v_0 \\ V \end{pmatrix}\right).
\end{aligned}$$

Equation (2.37) is a variational formulation for $(u_{\text{int}}, U)^\top \in H^1(\Omega_{\text{int}}) \times H^+(D)$ where $H^1(\Omega_{\text{int}})$ is the Sobolev space of weakly differentiable functions in Ω_{int}. For the trigonometric monomials $t^k(z) := \exp(ikz)$, $A(t^j, t^k) = \delta_{j,k}$. Thus, the implementation of the exterior part of B is reduced to the implementation of the two operators $\mathbf{T}^+$ and $\mathbf{T}^{(-)} : \mathbb{C} \times H^+(D) \to H^+(D)$.

If the ansatz space $\{t^0, t^1, ..., t^L\}$ is used for $H^+(D)$, these operators can be discretized by two matrices:

$$\mathcal{T}_L^{\pm} := \frac{1}{2}\begin{pmatrix} 1 & \pm 1 & & & \\ & 1 & \pm 1 & & \\ & & \ddots & \ddots & \\ & & & 1 & \pm 1 \\ & & & & 1 \end{pmatrix}. \tag{2.38}$$

The implementation of $\int_{x_r}^\infty \partial_x u_{\text{ext}}(x)\partial_x v_{\text{ext}}(x)dx$ is then done by the simple matrix matrix multiplication $2s_0\mathcal{T}_L^{(+)\top}\mathcal{T}_L^{(+)}$ and the implementation of $\int_{x_r}^\infty u_{\text{ext}}(x)v_{\text{ext}}(x)dx$ can be rephrased as $\frac{2}{s_0}\mathcal{T}_L^{(-)\top}\mathcal{T}_L^{(-)}$. These matrices are easily verified to correspond

to $A_{\text{ext}}^{\text{loc}}$ and $B_{\text{ext}}^{\text{loc}}$ that were derived in the previous section. However it will be useful in the next section to have the discrete correspondence of $\mathcal{T}_L^{(-)}$ to $\mathcal{L}_D\{u_{\text{ext}}\}(\widetilde{s})$ and of $\mathcal{T}_L^{(+)}$ to $\mathcal{L}_D\{\partial_x f\}(\widetilde{s})$.

In terms of $\mathcal{T}_L^{\pm}$, we can rewrite the equations for the exterior degrees of freedom, Equation (2.30) and Equation (2.31) as

$$A_{\text{ext}} = 2s_0 P_l^\top (\mathcal{T}_L^{(+)\top} \mathcal{T}_L^{(+)}) P_l + 2s_0 P_r^\top (\mathcal{T}_L^{(+)\top} \mathcal{T}_L^{(+)}) P_r \text{ and} \tag{2.39}$$

$$B_{\text{ext}} = \frac{2n_l^2}{s_0} P_l^\top (\mathcal{T}_L^{(-)\top} \mathcal{T}_L^{(-)}) P_l + \frac{2n_r^2}{s_0} P_r^\top (\mathcal{T}_L^{(-)\top} \mathcal{T}_L^{(-)}) P_r. \tag{2.40}$$

As before P_l and P_r are $L \times N$ matrices mapping the local degrees of freedom for the exterior domain to the global degrees of freedom.

2.4. Generalization to Higher Space Dimensions. The steps towards an extension of the method to two-dimensional space:

1. Subdivide the exterior domain Ω_{ext} into trapezoids that have one edge on Γ, the boundary of Ω_{int} and one edge infinitely far from it,
2. Map these trapezoids onto a reference strip, to obtain a coordinate transform,
3. Transform the variational formulation into the new coordinates,
4. Decouple the equations on the reference strip to obtain bounded integrals in the coordinate alongside the boundary of Ω_{int} and infinite integrals in the normal direction,
5. Treat bounded integrals with standard quadrature formulas,
6. Transform infinite integrals to $H^+(D)$ and use same discretization as in the one-dimensional case.

The mapping onto the reference rectangle in step 2 will give us coordinates (ξ, η), where ξ acts as a distance variable that measures the distance in the outward normal direction of Ω_{int}. Using this mapping we can transform the integrals in the variational formulation of our equation on a trapezoid onto a semi-infinite reference rectangle $[0,1] \times [0,\infty)$. Using Fubini's theorem, we can decouple the integrals on the reference strip in step 4. However, after decoupling the infinite integrals will contain multiplication with the integration variable ξ alongside the test and ansatz functions and their gradients in the integrand. This is a situation that was not covered before and makes step 6 more involved than the one-dimensional equivalent. It necessitates the definition of a new operator $\mathbf{D}$ which we will derive at the end of this section. Together with the operators $\mathbf{T}^{(+)}$ and $\mathbf{T}^{(-)}$ from the previous section, we will then be able to express all the integral expressions that appear in our formulation. We will also give the discrete form $\mathcal{D}_L$ of $\mathbf{D}$ when using the trigonometric monomials as basis for $H^+(D)$. Together with $\mathcal{T}_L^{(+)}$ and $\mathcal{T}_L^{(-)}$ defined in the previous section, this will enable us to discretize all the integrals occurring in the two-dimensional implementation of the pole condition.

As described by Ruprecht et al. [17] and Nannen and Schädle [14], the basic idea for an implementation in higher space dimensions is to use tensor product elements. Equation (2.1) for higher space dimensions takes the form

$$\Delta u(x) + n(x)^2 \omega^2 u(x) = 0 \quad for \quad x \in \Omega \tag{2.41}$$

where $\Omega \subseteq \mathbb{R}^n$, $n \in \{2,3\}$. Again, Ω is assumed to be unbounded and we divide the domain of interest into a bounded interior Ω_{int} and an unbounded exterior part Ω_{ext}.

Our approach is to assume a standard boundary condition at $\partial\Omega$ and the pole condition as radiation condition for the generalized radial part of u. An arbitrary convex polygon P is used to split the domain into $\Omega_{\text{int}} := \Omega \cap P$ and $\Omega_{\text{ext}} := \Omega \backslash P$. Ω_{int} and Ω_{ext} share the common boundary $\Gamma := \partial P$. While in the interior, $H^1(\Omega_{\text{int}})$ is treated with standard finite elements, we apply a segmentation of Ω_{ext} into infinite trapezoids in the two-dimensional case and infinite prismatiods in the three-dimensional case, see Fig. 2.4. In order for such a segmentation to be valid, we require $n(x)$ to be constant within each trapezoid or prismatoid. See [11, 19] for details on obtaining such a segmentation. We will stick to the two-dimensional case in the following paragraphs.

For the implementation we first need an affine bilinear mapping between a reference strip and each trapezoid, see Fig. 2.4. This mapping is a composition of three mappings, a transformation $T : (\xi, \eta) \to (x, y)$ that takes the reference strip to the right coordinate system, stretches and distorts it appropriately. T is followed by a rotation R around $(0, 0)$ and a shift $S : (x, y) \to (x, y) + P_1$.

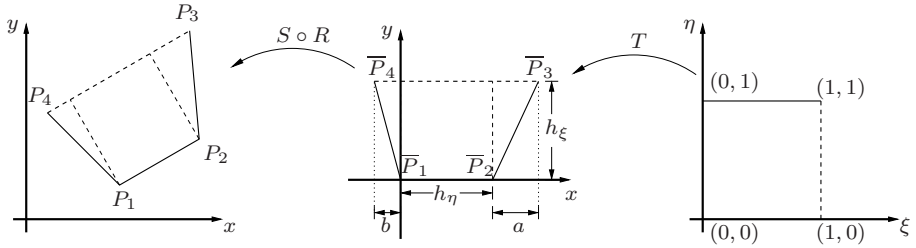

FIG. 2.4. *Mapping of the reference strip to an trapezoid. We have* $T(0,0) = \overline{P}_1$, $T(0,1) = \overline{P}_2$, $T(1,0) = \overline{P}_4$ *and* $T(1,1) = \overline{P}_3$ *and* $R(\overline{P}_i) = P_i$ *for* $i = 1, ..., 4$.

This mapping is given by

$$\begin{aligned}(x, y) &= (S \circ R \circ T)(\xi, \eta) \\ &= \frac{1}{\|P_2 - P_1\|} \begin{pmatrix} x_2 - x_1 & y_1 - y_2 \\ y_2 - y_1 & x_2 - x_1 \end{pmatrix} \begin{pmatrix} h_\eta \eta - b\xi + (a + b)\xi\eta \\ h_\xi \xi \end{pmatrix} + \begin{pmatrix} x_1 \\ y_1 \end{pmatrix}.\end{aligned} \tag{2.42}$$

The Jacobi matrix J of (2.42) and its determinant are

$$J = \begin{pmatrix} h_\eta + (a + b)\xi & -b + (a + b)\eta \\ 0 & h_\xi \end{pmatrix}, \quad |J| = h_\xi(h_\eta + (a + b)\xi). \tag{2.43}$$

Its inverse is

$$J^{-1} = \begin{pmatrix} \frac{1}{h_\eta + (a+b)\xi} & \frac{b - (a+b)\eta}{h_\xi(h_\eta + \xi(a+b))} \\ 0 & \frac{1}{h_\xi} \end{pmatrix} \tag{2.44}$$

We are now in a position to derive a suitable variational formulation of the exterior part of our problem. First we will transform the integrals over T onto the reference rectangle. On T the integrals read:

$$\int_T (\nabla u(x, y)) \cdot (\nabla v(x, y))\, d(x, y) + \omega^2 \int_T n(x, y)^2 u(x, y) v(x, y) d(x, y) = 0$$

Transforming to the reference rectangle, the test and ansatz function and refractive index transform as follows: $v(x, y) \to \hat{v}(\xi, \eta)$, $u(x, y) \to \hat{u}(\xi, \eta)$ and $n(x, y) \to \hat{n}(\xi, \eta)$.

We can factorize $\hat{u}(\xi,\eta) = \hat{u}_\xi(\xi)\hat{u}_\eta(\eta)$ and $\hat{v}(\xi,\eta) = \hat{v}_\xi(\xi)\hat{v}_\eta(\eta)$. Using this factorization, the transformed integrals decouple to independent integrals over ξ and η. Since the determinant $|J|$ is independent of η, by Fubini's theorem, we have

$$n_i^2 \int_T u(x,y)v(x,y)d(x,y) = n_i^2 \left(\int_0^1 \hat{u}_\eta(\eta)\hat{v}_\eta(\eta)d\eta\right)\left(\int_0^\infty \hat{u}_\xi(\xi)\hat{v}_\xi(\xi)|J|d\xi\right). \quad (2.45)$$

Due to the presence of $J^{-\top}$, the situation for the stiffness matrix is more involved. Inserting the definitions of J and the factorization of u and v yields

$$\begin{aligned}
&\int_T (\nabla u(x,y)) \cdot (\nabla v(x,y))\, d(x,y) \quad (2.46)\\
&= \left(\int_0^1 \hat{u}'_\eta(\eta)(h_\xi^2 + (b-(a+b)\eta)^2)\hat{v}'_\eta(\eta)d\eta\right)\left(\int_0^\infty \frac{\hat{u}_\xi(\xi)\hat{v}_\xi(\xi)}{h_\xi(h_\eta+(a+b)\xi)}d\xi\right)\\
&\quad + \left(\int_0^1 \hat{u}'_\eta(\eta)\frac{b-(a+b)\eta}{h_\xi}\hat{v}_\eta(\eta)d\eta\right)\left(\int_0^\infty \hat{u}_\xi(\xi)\hat{v}'_\xi(\xi)d\xi\right)\\
&\quad + \left(\int_0^1 \hat{u}_\eta(\eta)\frac{b-(a+b)\eta}{h_\xi}\hat{v}'_\eta(\eta)d\eta\right)\left(\int_0^\infty \hat{u}'_\xi(\xi)\hat{v}_\xi(\xi)d\xi\right)\\
&\quad + \left(\int_0^1 \hat{u}_\eta(\eta)\hat{v}_\eta(\eta)d\eta\right)\left(\int_0^\infty \hat{u}'_\xi(\xi)\frac{h_\eta+(a+b)\xi}{h_\xi}\hat{v}'_\xi(\xi)d\xi\right).
\end{aligned}$$

Suppose, that the interior Ω_{int} is already discretized with standard finite elements. Then the integrals alongside Γ, that is the bounded η-integrals, are discretized using the traces of the finite element basis functions in Ω_{int} on Γ as basis functions in η-direction, yielding matrices $T^{\text{ext}}_{\text{loc},i,1}$ to $T^{\text{ext}}_{\text{loc},i,5}$ in order of their appearance in Equations (2.45) and (2.46). We will now transform the infinite ξ-integrals to the Hardy space $H^+(D)$ using the techniques presented in the previous section. However, two of these integrals contain factors $(\xi+c)$ and $(\xi+c)^{-1}$ for constant $c>0$ that appear in the integrands. These factors are new in the higher-dimensional implementation and have to be dealt with separately. The next section will sketch a way to discretize the integrals containing these factors.

Including the argument s of $f(s)$ for clarity, we know from the basic properties of the Laplace transform that $\mathcal{L}\{sf(s)\}(\widetilde{s}) = -(\mathcal{L}\{f(s)\})'(\widetilde{s})$ and $\mathcal{L}\left\{\frac{f(s)}{s}\right\}(\widetilde{s}) = \int_0^\infty \mathcal{L}\{f\}(\sigma)d\sigma$. Using these properties, we can derive an operator $\mathbf{D} : H^+(D) \to H^+(D)$ for the factor ξ in Equation (2.46). Taking the equations to $H^+(D)$, we can implicitly define the operator $\mathbf{D}$ by

$$\mathbf{D}\left(\mathcal{M}_{s_0}\mathcal{L}\{f\}\right)(\widetilde{s}) = \mathcal{M}_{s_0}(-(\mathcal{L}\{f\})')(\widetilde{s}) = \mathcal{M}_{s_0}\mathcal{L}\{sf\}(\widetilde{s}). \quad (2.47)$$

For $F \in H^+(D)$, we can compute

$$(\mathbf{D}F)(\widetilde{s}) = \frac{(\widetilde{s}-1)^2}{2s_0}F'(\widetilde{s}) + \frac{\widetilde{s}-1}{2s_0}F(\widetilde{s}). \quad (2.48)$$

As in the one-dimensional case, we use the trigonometric monomials $t^k(z) := \exp(ikz)$ up to order L as basis of $H^+(D)$ then $\mathcal{D}_L$, the discrete form of $\mathbf{D}$ reads $\frac{1}{2s_0}\mathcal{D}_L$ with the matrix

$$\mathcal{D}_L := \begin{pmatrix} -1 & 1 & & & \\ 1 & -3 & 2 & & \\ & \ddots & \ddots & \ddots & \\ & & L & -2L-1 \end{pmatrix}. \quad (2.49)$$

A factor $(\xi + c)\hat{f}(\xi)$ in the integrand thus corresponds to the discrete $(\frac{1}{2s_0}\mathcal{D}_L + c\,\mathrm{id})(\mathcal{L}_D\{f\})$. For the factors $(\xi + c)^{-1}$, we use the fact, that they are the inverse of $(\xi + c)$, hence they can be discretized as $\left(\frac{1}{2s_0}\mathcal{D}_L + c\,\mathrm{id}\right)^{-1}(\mathcal{L}_D\{f\})$.

We are now in a position to give the matrices that are the discrete implementations of the infinite ξ-integrals in (2.45) and (2.46):

$$\begin{aligned}
\int_0^\infty \hat{u}_\xi(\xi)\hat{v}_\xi(\xi)|J|d\xi &= \int_0^\infty \hat{u}_\xi(\xi)\hat{v}_\xi(\xi)h_\xi(h_\eta + (a+b)\xi)d\xi \\
&\approx -\frac{2h_\xi}{s_0}\mathcal{T}_L^{(-)\top}\left(h_\eta\,\mathrm{id} + \frac{a+b}{2s_0}\mathcal{D}_L\right)\mathcal{T}_L^{(-)}, \\
\int_0^\infty \frac{\hat{u}_\xi(\xi)\hat{v}_\xi(\xi)}{h_\xi(h_\eta + (a+b)\xi)}d\xi &\approx -\frac{2}{s_0 h_\xi}\mathcal{T}_L^{(-)\top}\left(h_\eta\,\mathrm{id} + \frac{a+b}{2s_0}\mathcal{D}_L\right)^{-1}\mathcal{T}_L^{(-)}, \\
\int_0^\infty \hat{u}_\xi(\xi)\hat{v}'_\xi(\xi)d\xi &\approx -2\mathcal{T}_L^{(-)\top}\mathcal{T}_L^{(+)}, \\
\int_0^\infty \hat{u}'_\xi(\xi)\hat{v}_\xi(\xi)d\xi &\approx -2\mathcal{T}_L^{(+)\top}\mathcal{T}_L^{(-)} \text{ and} \\
\int_0^\infty \hat{u}'_\xi(\xi)\frac{h_\eta + (a+b)\xi}{h_\xi}\hat{v}'_\xi(\xi)d\xi &\approx -\frac{2s_0}{h_\xi}\mathcal{T}_L^{(+)\top}\left(h_\eta\,\mathrm{id} + \frac{a+b}{2s_0}\mathcal{D}_L\right)\mathcal{T}_L^{(+)}.
\end{aligned}$$

Thus, using $T^{\mathrm{ext}}_{\mathrm{loc}i}$ for the tangetial η-integrals, on the ith prismatoid T_i we have the following local stiffness matrix $A^{\mathrm{ext}}_{\mathrm{loc},i}$ and mass matrix $B^{\mathrm{ext}}_{\mathrm{loc},i}$:

$$\begin{aligned}
A^{\mathrm{ext}}_{\mathrm{loc},i} := {} & T^{\mathrm{ext}}_{\mathrm{loc},i,2} \otimes \left[\frac{-2h_\xi}{s_0}\mathcal{T}_L^{(-)\top}\left(h_\eta\,\mathrm{id} + \frac{a+b}{2s_0}\mathcal{D}_L\right)^{-1}\mathcal{T}_L^{(-)}\right] \\
& + T^{\mathrm{ext}}_{\mathrm{loc},i,3} \otimes \left[(-2)\mathcal{T}_L^{(-)\top}\mathcal{T}_L^{(-)}\right] + T^{\mathrm{ext}}_{\mathrm{loc},i,4} \otimes \left[(-2)\mathcal{T}_L^{(+)\top}\mathcal{T}_L^{(+)}\right] \\
& + T^{\mathrm{ext}}_{\mathrm{loc},i,5} \otimes \left[\frac{-2s_0}{h_\xi}\mathcal{T}_L^{(+)\top}\left(h_\eta\,\mathrm{id} + \frac{a+b}{2s_0}\mathcal{D}_L\right)\mathcal{T}_L^{(+)}\right] \text{ and} \qquad (2.50) \\
B^{\mathrm{ext}}_{\mathrm{loc},i} := {} & n_i^2 T^{\mathrm{ext}}_{\mathrm{loc},i,1} \otimes \left[\frac{-2h_\xi}{s_0}\mathcal{T}_L^{(-)\top}\left(h_\eta\,\mathrm{id} + \frac{a+b}{s_0}\mathcal{D}_L\right)\mathcal{T}_L^{(-)}\right]. \qquad (2.51)
\end{aligned}$$

If as in the previous sections, P_i denotes the L by N matrix mapping the local degrees of freedom to global degrees of freedom, we obtain the exterior part A_{ext} and B_{ext} of the matrices A and B by summing over all trapezoids:

$$A_{\mathrm{ext}} = \sum_{T_i} P_i^\top A^{\mathrm{ext}}_{\mathrm{loc},i} P_i \text{ and } B_{\mathrm{ext}} = \sum_{T_i} P_i^\top B^{\mathrm{ext}}_{\mathrm{loc},i} P_i. \qquad (2.52)$$

Since each segment in Ω_{ext} is treated separately, it is possible to account for unbounded inhomogeneities such as waveguides. This does not require any further implementation but can be dealt with by the methods presented here. The exact statement of the tensor product spaces and the right test functions are quite technical and can be found in great detail in [8] and [12].

3. Detecting Spurious Solutions. Since our assumption is that spurious solutions are caused by badly converged solutions in the exterior domain, it is likely that they will respond more strongly to perturbations of this exterior domain than

the physical solutions. We will make use of these findings by presenting a method for detecting the spurious solutions within the computed eigenvalue spectrum. Our idea is to investigate the dependence of the eigenvalues with respect to the pole condition parameter s_0.

Since the reaction of quantities of interest to perturbations is typically determined by condition numbers, we will first attempt to detect spurious solutions using the condition numbers of the eigenvalues of the generalized eigenvalue problem. This does not make use of the fact that we need not deal with an arbitrary perturbation but with a perturbation that is well-defined. This will allow us to directly compute the reaction of the eigenvalues to variations of the pole condition parameter s_0. Finally we will investigate the domains of convergence for our method that will allow us to implement a convergence monitor that gives us regions where the statements derived in this chapter produce reliable results.

The discretization of a resonance problem with finite elements in the interior and the pole condition in the exterior leads to a generalized eigenvalue problem $(A - \omega B)\mathbf{u} = 0$ or equivalently $(\beta A - \alpha B)\mathbf{u} = 0$. The matrix pairs (A, B) that we will have to deal with are regular, that is there exists a pair $\langle\alpha, \beta\rangle$ that we refer to as *eigenvalue* of the problem, such that $\det(\beta A - \alpha B) \neq 0$. As a consequence, there is an established perturbation theory which is applicable to our problem [20, 22, 21]. The perturbation theory of our problem would drastically simplify, if we could rewrite $A\mathbf{u} = \omega B\mathbf{u}$ in the form $B^{-1}A\mathbf{u} = \omega\mathbf{u}$. Then we would have reduced the generalized Eigenvalue problem to an ordinary eigenvalue problem, however, since B is singular or ill-conditioned in our application, this reduction is not possible.

3.1. Condition Numbers and Direct Perturbations. Let (A, B) be a complex matrix pair of order n and $(\widetilde{A}, \widetilde{B}) := (A + \Delta A, B + \Delta B)$ be the perturbed pair with perturbations ΔA and ΔB. Then a first order expansion for the eigenvalues of the perturbed system is given by the literature as follows:

THEOREM 3.1. *Let* $\mathbf{u}$ *and* $\mathbf{v}$ *be the right and left eigenvectors for the simple eigenvalue* $\langle\alpha, \beta\rangle = \langle \mathbf{v}^H A\mathbf{u}, \mathbf{v}^H B\mathbf{u}\rangle$ *of the regular matrix pair* (A, B)*. Let* $(\widetilde{A}, \widetilde{B}) = (A + \Delta A, B + \Delta B)$ *be the perturbed pair,* $\varepsilon = \sqrt{\|\Delta A\|_2^2 + \|\Delta B\|_2^2}$ *and* $\langle\widetilde{\alpha}, \widetilde{\beta}\rangle$ *be the perturbed eigenvalue corresponding to* $\langle\alpha, \beta\rangle$*. Then*

$$\langle\widetilde{\alpha}, \widetilde{\beta}\rangle = \langle\alpha + \mathbf{v}^H \Delta A\mathbf{u}, \beta + \mathbf{v}^H \Delta B\mathbf{u}\rangle + \mathcal{O}(\varepsilon^2). \tag{3.1}$$

Proof. A proof can be found e.g. at [21, Theorem 4.12]. ∎

This result allows us to compute the relative condition number of an eigenvalue. First using $\alpha = \mathbf{v}^H A\mathbf{u}$, $\beta = \mathbf{v}^H B\mathbf{u}$, $\widetilde{\alpha} = \alpha + \mathbf{v}^H \Delta A\mathbf{u}$ and $\widetilde{\beta} = \beta + \mathbf{v}^H \Delta B\mathbf{u}$, we may compute the chordal distance $\mathcal{X}(\langle\alpha, \beta\rangle, \langle\widetilde{\alpha}, \widetilde{\beta}\rangle)$ between $\langle\alpha, \beta\rangle$ and $\langle\widetilde{\alpha}, \widetilde{\beta}\rangle$:

$$\mathcal{X}(\langle\alpha, \beta\rangle, \langle\widetilde{\alpha}, \widetilde{\beta}\rangle) = \frac{|\alpha\widetilde{\beta} - \beta\widetilde{\alpha}|}{\sqrt{|\alpha|^2 + |\beta|^2}\sqrt{|\widetilde{\alpha}|^2 + |\widetilde{\beta}|^2}} \approx \frac{|\alpha\mathbf{v}^H \Delta B\mathbf{u} - \beta\mathbf{v}^H \Delta Ax|}{|\alpha|^2 + |\beta|^2} \tag{3.2}$$

The numerator in equation (3.2) can be rewritten as

$$|\alpha\mathbf{v}^H \Delta B\mathbf{u} - \beta\mathbf{v}^H \Delta A\mathbf{u}| = \left|(\alpha, \beta)\begin{pmatrix}\mathbf{v}^H \Delta B\mathbf{u} \\ -\mathbf{v}^H \Delta A\mathbf{u}\end{pmatrix}\right| \leq \varepsilon\|\mathbf{u}\|_2\|\mathbf{v}\|_2\sqrt{|\alpha|^2 + |\beta|^2}. \tag{3.3}$$

Inserting equation (3.3) into (3.2), we have

$$\mathcal{X}(\langle\alpha, \beta\rangle, \langle\widetilde{\alpha}, \widetilde{\beta}\rangle) \lesssim \frac{\|\mathbf{u}\|_2\|\mathbf{v}\|_2}{\sqrt{|\alpha|^2 + |\beta|^2}}\varepsilon. \tag{3.4}$$

This number acts as relative condition number of the eigenvalue $\kappa_{rel}(\langle\alpha,\beta\rangle)$. In order to obtain an implementation of this method, we solve the generalized eigenvalue problem $(A-\omega B)\mathbf{u}=0$ with the standard generalized sparse eigenvalue solver in MATLAB, which is an implementation of the Arnoldi method with spectral deformation. This produces the spectrum $\sigma(A,B)$ together with the right eigenvectors. Since a left eigenvector $\mathbf{v}$ satisfies $\mathbf{v}^H(A-\omega B)=0$, we can obtain $\mathbf{v}$ by solving the hermitian conjugate of the problem $(A^H-\overline{\lambda}B^H)\mathbf{v}=0$.

Since κ_{rel} is a relative condition number, we can expect higher eigenvalues to have lower condition numbers. This may seem unintuitive from a physical point of view since the approximation of higher eigenvalues is typically worse for a fixed grid. However from a purely algebraic viewpoint, this is in good agreement with the notion *relative condition number*. This means that lower physical modes may have higher condition numbers than higher order spurious solutions. In order to obtain a global criterion for the detection of spurious solutions, we have to compare condition numbers of eigenvalues that have a similar distance from the origin. We achieve that by rescaling our condition numbers with a factor $|\omega|$. However, numerical investigations showed that the use of condition numbers works for some examples but is generally unreliable. This is due to the fact, that the condition number is a purely algebraic feature that disregards all knowledge about the physics of the problem and about the nature of the perturbation. We will now aim at deriving a condition that is void of the generality of the condition number but includes the special knowledge about the kind of perturbation we cause when changing the pole condition parameter s_0. A way to obtain such a direct approximation stems from the backwards error analysis for the generalized eigenvalue problem [7]: Given the generalized eigenvalue problem, if we perturb the matrices A and B by ΔA and ΔB, this results in perturbed eigenvalue $\Delta\omega$, right eigenvector $\Delta\mathbf{u}$ and left eigenvector $\Delta\mathbf{v}$. Since ΔA and ΔB arise from a variation of the pole condition parameter s_0, we know them explicitly, which will allow us to compute $\Delta\omega$ directly.

LEMMA 3.2. *Let* $\mathbf{u}$ *and* $\mathbf{v}$ *be the left and right eigenvectors for the eigenvalue* ω *of the generalized eigenvalue problem* $(A-\omega B)\mathbf{u}=0$. *Let* ΔA *and* ΔB *be perturbations of* A *and* B. *This leads to perturbed eigenvalue* $\omega+\Delta\omega$ *and eigenvectors* $\mathbf{u}+\Delta\mathbf{u}$ *and* $\mathbf{v}+\Delta\mathbf{v}$. *Then in first order we can approximate* $\Delta\omega$ *by*

$$\Delta\omega=\frac{\mathbf{v}^H\Delta A\mathbf{u}-\omega\mathbf{v}^H\Delta B\mathbf{u}}{\mathbf{v}^HB\mathbf{u}}+\mathcal{O}(\varepsilon^2). \tag{3.5}$$

Proof. Using the perturbed left and right eigenvectors arising from a perturbation of A and B and the perturbed eigenvalue, we rewrite the entire perturbed problem as

$$(A+\Delta A)(\mathbf{u}+\Delta\mathbf{u})=(\omega+\Delta\omega)(B+\Delta B)(\mathbf{u}+\Delta\mathbf{u}). \tag{3.6}$$

Next, we expand equation (3.6) and premultiply with $\mathbf{v}^H$, the left eigenvector for ω. Since $\mathbf{v}^HA=\omega\mathbf{v}^HB$, we can cancel some of the resulting terms and get

$$\begin{aligned}\mathbf{v}^H\Delta A\mathbf{u}+\mathbf{v}^H\Delta A\Delta\mathbf{u}&=\omega\mathbf{v}^H\Delta B\mathbf{u}+\omega\mathbf{v}^H\Delta B\Delta\mathbf{u} \\ +\Delta\omega\mathbf{v}^HB\mathbf{u}+\Delta\omega\mathbf{v}^HB\Delta\mathbf{u}&+\Delta\omega\mathbf{v}^H\Delta B\mathbf{u}+\Delta\omega\mathbf{v}^H\Delta B\Delta\mathbf{u}.\end{aligned} \tag{3.7}$$

Isolating $\Delta\omega$ in (3.7) and neglecting the higher order terms we arrive at the first order approximation of $\Delta\omega$:

$$\Delta\omega=\frac{\mathbf{v}^*\Delta A\mathbf{u}-\omega\mathbf{v}^*\Delta B\mathbf{u}}{\mathbf{v}^*B\mathbf{u}}+\mathcal{O}(\varepsilon^2). \tag{3.8}$$

□

Using the formula for $\Delta\omega$, we can directly compute the effect of a perturbation of the pole condition parameter on an eigenvalue $\omega \in \sigma(A, B)$. We know that the matrices A and B are dependent on s_0, the pole condition parameter. Our task is to find out the perturbed eigenvalue $\Delta\omega$ for a perturbation Δs_0 of s_0. That means, we need to compute the change in the matrices A and B, ΔA and ΔB. Since only the entries of the exterior, A_{ext} and B_{ext}, depend on s_0, all other entries cancel, if we compute ΔA and ΔB. We recall that for the one-dimensional case

$$A_{\text{ext}} = 2s_0 P_l^\top (\mathcal{T}_L^{(+)\top} \mathcal{T}_L^{(+)}) P_l + 2s_0 P_r^\top (\mathcal{T}_L^{(+)\top} \mathcal{T}_L^{(+)}) P_r \text{ and}$$
$$B_{\text{ext}} = \frac{2n_l^2}{s_0} P_l^\top (\mathcal{T}_L^{(-)\top} \mathcal{T}_L^{(-)}) P_l + \frac{2n_r^2}{s_0} P_r^\top (\mathcal{T}_L^{(-)\top} \mathcal{T}_L^{(-)}) P_r.$$

(cf. Equations (2.39) and (2.40)) and for the two-dimensional case

$$A_{\text{ext}} = \sum_{T_i} P_i^\top A_{\text{loc},i}^{\text{ext}} P_i \text{ and}$$
$$B_{\text{ext}} = \sum_{T_i} P_i^\top B_{\text{loc},i}^{\text{ext}} P_i.$$

So for the one-dimensional case, we can directly compute

$$\Delta A = 2\Delta s_0 \left(P_l^\top (\mathcal{T}_L^{(+)\top} \mathcal{T}_L^{(+)}) P_l + P_r^\top (\mathcal{T}_L^{(+)\top} \mathcal{T}_L^{(+)}) P_r \right) \text{ and}$$
$$\Delta B = -\frac{\Delta s_0}{s_0(s_0 + \Delta s_0)} \left(n_l^2 P_l^\top (\mathcal{T}_L^{(-)\top} \mathcal{T}_L^{(-)}) P_l + n_r^2 P_r^\top (\mathcal{T}_L^{(-)\top} \mathcal{T}_L^{(-)}) P_r \right).$$

For the two-dimensional case, we have by the same calculation

$$\Delta A = \Delta s_0 \sum_{T_i} P_i^\top A_{\text{loc},i}^{\text{ext},(1)} P_i - \frac{\Delta s_0}{s_0(s_0 + \Delta s_0)} \sum_{T_i} P_i^\top A_{\text{loc},i}^{\text{ext},(2)} P_i \text{ and}$$
$$\Delta B = -\frac{\Delta s_0}{s_0(s_0 + \Delta s_0)} n_i^2 \sum_{T_i} P_i^\top B_{\text{loc},i}^{\text{ext},(-1)} P_i - \frac{\Delta s_0 \left(2s_0 + \Delta s_0\right)}{\left(s_0 + \Delta s_0\right)^2 {s_0}^2} n_i^2 \sum_{T_i} P_i^\top B_{\text{loc},i}^{\text{ext},(-2)} P_i.$$

Again, we will have to introduce a scaling of $\Delta\lambda$, the quantity we will use to identify the spurious solutions. However, the scaling we will use differs from the scaling for the relative condition number. We established in Section 2.2, that the approximation of the Laplace transform of the exterior solution $\mathcal{L}\{u_{\text{ext}}\} \circ \mathcal{M}_{s_0}$ by an power series expansion will be best near s_0. Thus, it is reasonable to expect the resonances to be more sensitive to perturbations of s_0 with increasing distance to the parameter and the detection to be valid only for a certain region around s_0.

3.2. A Convergence Monitor for Resonances. The methods we derived in the previous sections for the detection of spurious solutions all suffer from the major drawback that it is not possible to distinguish between solutions that react strongly to perturbations (i.e. are ill-conditioned) because they are spurious solutions and modes that correspond to physical solutions but react strongly to perturbations because their approximation is not good enough in the exterior domain Ω_{ext}. In order to overcome this problem, we will complement the methods from the previous sections with a convergence monitor. This will give us a region in the complex plane in which

the eigenvalues are well-converged for our choice of s_0 and the number of degrees of freedom L used in the computation.

First we will analyze the situation in the one-dimensional case. We discard all other information and just look at one part of the exterior domain. There it holds that

$$2s_0\mathcal{T}_L^{(+)\top}\mathcal{T}_L^{(+)}\mathbf{u}_{\text{ext}} - \omega^2\frac{2n_{\text{ext}}^2}{s_0}\mathcal{T}_L^{(-)\top}\mathcal{T}_L^{(-)}\mathbf{u}_{\text{ext}} = 0, \tag{3.9}$$

where $\mathbf{u}_{\text{ext}}$ are the degrees of freedom for the respective part of the exterior domain and n_{ext} is the refractive index therein. Inserting the definitions of $\mathcal{T}_L^{(+)}$ and $\mathcal{T}_L^{(-)}$ from Equation (2.38), and naming the entries of $\mathbf{u}_{\text{ext}} = (z_0, z_1, \dots z_L)^\top$, the matrix form of Equation (3.9) reads:

$$s_0\begin{pmatrix} \frac{1}{2} & \frac{1}{2} & & \\ & \frac{1}{2} & 1 & \frac{1}{2} \\ & & \ddots & \end{pmatrix}\begin{pmatrix} z_0 \\ z_1 \\ \vdots \end{pmatrix} - \omega^2\frac{n_{\text{ext}}^2}{s_0}\begin{pmatrix} \frac{1}{2} & -\frac{1}{2} & & \\ & -\frac{1}{2} & 1 & -\frac{1}{2} \\ & & \ddots & \end{pmatrix}\begin{pmatrix} z_0 \\ z_1 \\ \vdots \end{pmatrix} = 0.$$

For $l \geq 3$, the matrix equation corresponds to a linear second order recurrence with coefficients depending on ω^2. Its characteristic polynomial is

$$\chi_{\omega^2}(z) = \left(\frac{s_0}{2} + \omega^2\frac{n_{\text{ext}}^2}{2s_0}\right)z^2 + \left(s_0 - \omega^2\frac{n_{\text{ext}}^2}{s_0}\right)z + \left(\frac{s_0}{2} + \omega^2\frac{n_{\text{ext}}^2}{2s_0}\right). \tag{3.10}$$

The roots of Equation (3.10) solve the recurrence relation and determine the stability of the solutions. They are $z_1 = (n_{\text{ext}}\omega + is_0)(n_{\text{ext}}\omega - is_0)^{-1}$ and $z_2 = (n_{\text{ext}}\omega - is_0)(n_{\text{ext}}\omega + is_0)^{-1}$. The convergence rate of the solution corresponding to z_i^k is given by $|z_i^{k+1}| = \kappa|z_i^k|$, hence $\kappa = \frac{|z_i^{k+1}|}{|z_i^k|} = |z_i|$. Clearly it holds that $z_1 z_2 = 1$, hence, if the solution corresponding to z_1 is asymptotically stable, the solution corresponding to z_2 diverges and vice versa. We can restrict ourselves to investigating the convergence behavior of the solution connected with z_2 which is the outward radiating solution. In order that the solution converges with a convergence rate $0 < \kappa < 1$, we require that $|z_2| = \kappa$, hence $|n_{\text{ext}}\omega - is_0| = \kappa|n_{\text{ext}}\omega + is_0|$. This can be reformulated

$$\left(\frac{n_{\text{ext}}\omega}{is_0} - 1\right)\overline{\left(\frac{n_{\text{ext}}\omega}{is_0} - 1\right)} = \kappa^2\left(\frac{n_{\text{ext}}\omega}{is_0} + 1\right)\overline{\left(\frac{n_{\text{ext}}\omega}{is_0} + 1\right)}$$

By splitting real and imaginary part of ${}^{n_{\text{ext}}\omega}/_{is_0}$, expanding the quadratic terms, dividing by $1-\kappa^2$ and completing the square, we obtain

$$\left[\Re\left(\frac{n_{\text{ext}}\omega}{is_0}\right) - \frac{1+\kappa^2}{1-\kappa^2}\right]^2 + \Im\left(\frac{n_{\text{ext}}\omega}{is_0}\right)^2 = \left(\frac{1+\kappa^2}{1-\kappa^2}\right)^2 - 1. \tag{3.11}$$

Since $(\Re(a)-b)^2+\Im(a)^2 = (\Re(a)-b)^2-(i\Im(a))^2 = (\Re(a)+i\Im(a)-b)(\Re(a)-i\Im(a)-b)$, we can isolate ω in Equation (3.11) and derive the domain C where the series converges with a convergence rate of κ to be

$$C = \left\{\omega \in \mathbb{C} : \left|\omega n_{\text{ext}} - is_0\frac{1+\kappa^2}{1-\kappa^2}\right| \leq |is_0|\sqrt{\left(\frac{1+\kappa^2}{1-\kappa^2}\right)^2 - 1}\right\}. \tag{3.12}$$

We will now generalize to higher space dimensions. In order to obtain a formulation that we are able to deal with, we will investigate the simpler case where the infinite edges of the prismatoid are parallel and perpendicular to the boundary of Ω_{int}, that is $a = b = 0$ in Equations (2.50) and (2.51). This will give us the simpler local stiffness and mass matrices

$$\begin{aligned} A^{\text{ext}}_{\text{loc},i} &= T^{\text{ext}}_{\text{loc},i,2} \otimes \left[\frac{-2h_\xi}{h_\eta s_0} \mathcal{T}_L^{(-)\top} \mathcal{T}_L^{(-)} \right] + T^{\text{ext}}_{\text{loc},i,3} \otimes \left[(-2) \mathcal{T}_L^{(-)\top} \mathcal{T}_L^{(+)} \right] \\ &\quad + T^{\text{ext}}_{\text{loc},i,4} \otimes \left[(-2) \mathcal{T}_L^{(+)\top} \mathcal{T}_L^{(-)} \right] + T^{\text{ext}}_{\text{loc},i,5} \otimes \left[\frac{-2h_\eta s_0}{h_\xi} \mathcal{T}_L^{(+)\top} \mathcal{T}_L^{(+)} \right] \text{ and} \\ B^{\text{ext}}_{\text{loc},i} &= n_i^2 T^{\text{ext}}_{\text{loc},i,1} \otimes \left[\frac{-2h_\xi h_\eta}{s_0} \mathcal{T}_L^{(-)\top} \mathcal{T}_L^{(-)} \right]. \end{aligned} \tag{3.13}$$

Due to the absence of $\mathcal{D}_L$, both matrices now have a tridiagonal structure. Moreover, for our simplified setting the finite integrals $T^{\text{ext}}_{\text{loc},i,3}$ and $T^{\text{ext}}_{\text{loc},i,4}$ are zero. Also in order for our discretization with prismatiods to be valid for the case of parallel infinite sides, we set $h_\xi = 1$, leaving h_η, which on the ith prismatoid we will index as $h_{\eta,i}$, to determine the coupling of the two infinite sides of each prismatoid. Putting it all together, we can give discrete ξ-directional part of the local infinite element stiffness matrix $A^{\text{ext}}_{\text{loc},i}$ as

$$A^{\text{ext}}_{\text{loc},i} = T^{\text{ext}}_{\text{loc},i,2} \otimes \left[\frac{(-2)}{h_{\eta,i} s_0} \mathcal{T}_L^{(-)\top} \mathcal{T}_L^{(-)} \right] + T^{\text{ext}}_{\text{loc},i,5} \otimes \left[(-2) h_{\eta,i} s_0 \mathcal{T}_L^{(+)\top} \mathcal{T}_L^{(+)} \right].$$

and the local infinite element mass matrix $B^{\text{ext}}_{\text{loc},i}$ as

$$B^{\text{ext}}_{\text{loc},i} = n_i^2 T^{\text{ext}}_{\text{loc},i,1} \otimes \left[\frac{(-2) h_{\eta,i}}{s_0} \mathcal{T}_L^{(-)\top} \mathcal{T}_L^{(-)} \right].$$

If we choose finite edge elements to discretize the interior Ω_{int}, then the traces of these elements on the boundary Γ between Ω_{int} and Ω_{ext} are standard one-dimensional finite elements and $T^{\text{ext}}_{\text{loc},i,1}$, $T^{\text{ext}}_{\text{loc},i.2}$ and $T^{\text{ext}}_{\text{loc},i,5}$ are the standard one-dimensional finite element matrices. Using linear finite edge elements in the interior and inserting the well-known one-dimensional matrices for the boundary integrals, the local infinite element stiffness matrix $A^{\text{ext}}_{\text{loc},i}$ is

$$\begin{aligned} A^{\text{ext}}_{\text{loc},i} = &\frac{1}{h_{\eta,i} s_0} \begin{pmatrix} (-2) \left[\mathcal{T}_L^{(-)\top} \mathcal{T}_L^{(-)} \right] & 2 \left[\mathcal{T}_L^{(-)\top} \mathcal{T}_L^{(-)} \right] \\ 2 \left[\mathcal{T}_L^{(-)\top} \mathcal{T}_L^{(-)} \right] & (-2) \left[\mathcal{T}_L^{(-)\top} \mathcal{T}_L^{(-)} \right] \end{pmatrix} + \\ &\frac{h_{\eta,i} s_0}{6} \begin{pmatrix} (-4) \left[\mathcal{T}_L^{(+)\top} \mathcal{T}^{(+)} \right] & (-2) \left[\mathcal{T}_L^{(+)\top} \mathcal{T}_L^{(+)} \right] \\ (-2) \left[\mathcal{T}_L^{(+)\top} \mathcal{T}_L^{(+)} \right] & (-4) \left[\mathcal{T}_L^{(+)\top} \mathcal{T}_L^{(+)} \right] \end{pmatrix}. \end{aligned} \tag{3.14}$$

The local infinite element mass matrix $B^{\text{ext}}_{\text{loc},i}$ is

$$B^{\text{ext}}_{\text{loc},i} = \frac{n_i^2 h_{\eta,i}}{6 s_0} \begin{pmatrix} (-4) \left[\mathcal{T}_L^{(-)\top} \mathcal{T}^{(-)} \right] & (-2) \left[\mathcal{T}_L^{(-)\top} \mathcal{T}_L^{(-)} \right] \\ (-2) \left[\mathcal{T}_L^{(-)\top} \mathcal{T}_L^{(-)} \right] & (-4) \left[\mathcal{T}_L^{(-)\top} \mathcal{T}_L^{(-)} \right] \end{pmatrix}. \tag{3.15}$$

In order to carry out a convergence analysis that is similar to the one-dimensional approach, we will now reformulate the two-dimensional problem as linear second order

matrix recurrence relation. We have established before in Equations (3.14) and (3.15) that both $A^{\text{ext}}_{\text{loc},i}$ and $B^{\text{ext}}_{\text{loc},i}$ consist of two coupled tri-diagonal block matrices for each trapezoid, dividing the corresponding vector of unknowns into two blocks. Each of these blocks corresponds to one infinite side of the trapezoid. Since each infinite ray is the boundary of two prismatoids, each of these tri-diagonal block matrices couples with two other blocks. The unknowns $\mathbf{u}_{N+iL}, ...\mathbf{u}_{N+(i+1)L-1}, i \in \{0, ..., k\}$ correspond to the Hardy modes on the ith infinite ray. In order to obtain a formulation that allows for a similar treatment as the one-dimensional situation and allows for computation of a domain of convergence, we will now collect the degrees of freedom that correspond to the same Hardy mode on each ray. That is, for $m \in \{0, ..., L-1\}$ we will create a vector that collects the unknowns corresponding to the mth Hardy modes on each ray:

$$\mathbf{u}^{(m)}_{\text{ext}} = (\mathbf{u}_{N+m}, \mathbf{u}_{N+L+m}, \mathbf{u}_{N+2L+m}, ..., \mathbf{u}_{N+kL+m})^\top. \tag{3.16}$$

The unknown $\mathbf{u}_{N+iL+m}$ is related with two neighboring unknowns $\mathbf{u}_{N+iL+m-1}$ and $\mathbf{u}_{N+iL+m+1}$ where $i \in \{0, ..., k\}$ and $m \in \{0, ..., L-1\}$. Naming the entries of the global stiffness matrix $\alpha_{i,j}$ and of the global mass matrix $\beta_{i,j}$, this relation is given by

$$\begin{aligned}(\alpha_{N+iL+m,N+iL+m-1} - n_i^2\omega^2\beta_{N+iL+m,N+iL+m-1})\mathbf{u}_{N+iL+m-1}\\ +(\alpha_{N+iL+m,N+iL+m} - n_i^2\omega^2\beta_{N+iL+m,N+iL+m})\ \mathbf{u}_{N+iL+m}\\ +(\alpha_{N+iL+m,N+iL+m+1} - n_i^2\omega^2\beta_{N+iL+m,N+iL+m+1})\mathbf{u}_{N+iL+m+1} = 0.\end{aligned}$$

However, since each infinite ray r_i couples with two other rays, r_j and r_l, we have such a relation for three different values of i in each row. Using the vectors $\mathbf{u}^{(m)}_{\text{ext}}$ defined in Equation (3.16), we have a linear second order matrix recurrence relation

$$M^{(0)}_\omega \mathbf{u}^{(m-1)}_{\text{ext}} + M^{(1)}_\omega \mathbf{u}^{(m)}_{\text{ext}} + M^{(2)}_\omega \mathbf{u}^{(m+1)}_{\text{ext}} = 0. \tag{3.17}$$

The coefficient matrices $M^{(0)}_\omega, M^{(1)}_\omega$ and $M^{(2)}_\omega$ are complex $k \times k$ matrices that depend on ω^2 and contain three nonzero entries composed of $\alpha_{i,j}$ and $\beta_{i,j}$ per row.

In order to be able to gain some insight about the stability of its solutions, we will transform it to a more convenient form by rephrasing it as linear first order matrix recurrence relation with a $2k \times 2k$ coefficient matrix . This is done by solving Equation (3.17) for $\mathbf{u}^{(m+1)}_{\text{ext}}$ and then concatenating the two vectors $\mathbf{u}^{(j+1)}_{\text{ext}}$ and $\mathbf{u}^{(j)}_{\text{ext}}$ into a vector:

$$\begin{aligned} 0 =& M^{(0)}_\omega \mathbf{u}^{(m-1)}_{\text{ext}} + M^{(1)}_\omega \mathbf{u}^{(m)}_{\text{ext}} + M^{(2)}_\omega \mathbf{u}^{(m+1)}_{\text{ext}} \\ \Leftrightarrow \qquad \begin{pmatrix} \mathbf{u}^{(m+1)}_{\text{ext}} \\ \mathbf{u}^{(m)}_{\text{ext}} \end{pmatrix} =& \underbrace{\begin{pmatrix} \left(-M^{(2)}_\omega\right)^{-1} M^{(1)}_\omega & \left(-M^{(2)}_\omega\right)^{-1} M^{(0)}_\omega \\ \text{id} & 0 \end{pmatrix}}_{=:C} \begin{pmatrix} \mathbf{u}^{(m)}_{\text{ext}} \\ \mathbf{u}^{(m-1)}_{\text{ext}} \end{pmatrix} \end{aligned}$$

As in the one-dimensional case, it is an established fact, that the stability of the solutions of a linear vector iteration $x_{n+1} = Cx_n$ with $A \in \mathbb{C}^{n\times n}$ depends on the corresponding eigenvalues of the coefficient matrix C (see e.g. [5, Theorem 3.33]). However, due to the inversion of $M^{(2)}_\omega$ and the computation of the eigenvalues of C, it is not possible to find a closed formula for the computation of the domain of convergence in the two-dimensional case. Instead, we will have to do a sampling for

different values of ω and compute the eigenvalues of C for each ω. That means for each value of ω, we compute the matrix C and its eigenvalues. This gives $2k$ eigenvalues for each ω. It can be seen however, that these $2k$ eigenvalues are clustered around two centers c_1 and c_2, one corresponding to an outgoing solution and one corresponding to an incoming solution. The two centers and the mean deviation from them can be computed using a kmeans algorithm. As in the one-dimensional case, the modulus of the eigenvalue corresponding to the outgoing solution determines the convergence rate of the solution. Even though the algorithmic computation of the convergence rate requires one matrix inversion and the computation of the eigenvalues of a matrix for each value of ω, its costs are moderate since the size of the matrices involved, k corresponds to the number of prismatoids used for the discretization of the exterior which is modest for typical applications.

4. Numerical Examples. We will start off with a simple one-dimensional cavity depicted in Figure 4.1 and using an ansatz with special functions, its resonances can be analytically computed to be $\omega = \frac{k\pi}{(x_r - x_l)n_i} - i\frac{1}{(x_r-x_l)n_i} \ln\left(\frac{n_i+n_e}{n_i-n_e}\right), \quad k \in \mathbb{N}$.

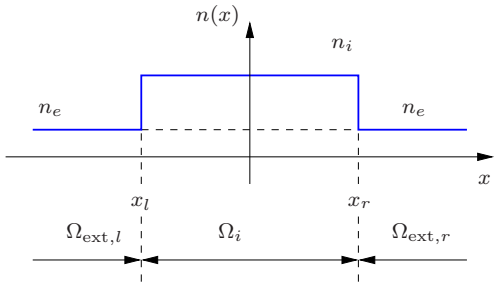

FIG. 4.1. *One-dimensional cavity layout.*

We set $n_{\text{int}} = \sqrt{2}$, $n_{\text{ext}} = 1$, $x_l = -1$ and $x_r = 1$. To obtain an numerical solution, we split $\mathbb{R}$ into $\Omega_{\text{int}} = [-2, 2]$ which contains the cavity and some surrounding air. The interior Ω_{int} was discretized with first order finite elements with an equidistant mesh with a mesh width $h = \frac{1}{45} \approx 0.022$. For the exterior we used the pole condition with $L = 15$ terms of the series expansion and a parameter value $s_0 = 0.4 - 1.0i$. The resonances computed by our algorithm are marked with dots in the left hand side image of Figure 4.2 while the analytically computed resonances are marked with squares. We then computed the weighted condition numbers for each resonance and collected them into clusters using a kmeans algorithm. The other symbols mark the cluster each resonance belongs to. We can see that all physical solutions belong to the first three clusters. In the right-hand side image of Figure 4.2, the resonances who respond to a perturbation of s_0 with a perturbation that is $\Delta\omega = \mathcal{O}(\Delta s_0)$ are marked. Again, they correspond with the physical resonances of the system. Hence for this simple model example, both methods for detecting spurious solutions will work.

Next we will look at another one-dimensional example. An air-filled cavity from $x = -1$ to $x = 1$ is surrounded by a cladding with a material with refractive index $n = 3.5$ and a thickness of $d = 1$ on each side which is embedded in an infinitely thick material with refractive index $n = 2.5$. The layout of this example is sketched in Figure 4.3.

In order to obtain a reference solution for this problem, we use the commercial FEM software package JCMSUITE [15, 23]. In the left-hand side image of Figure 4.4,

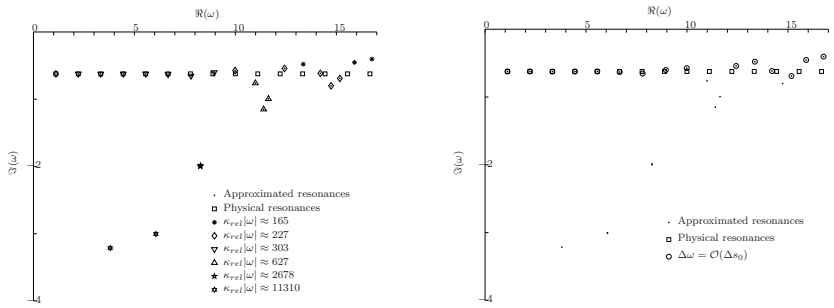

FIG. 4.2. *The spectrum $\sigma(A, B)$ of the first example in the left-hand figure, eigenvalues are marked corresponding to their weighted condition numbers, in the right-hand side figure eigenvalues with $\Delta\omega = \mathcal{O}(\Delta s_0)$ are marked.*

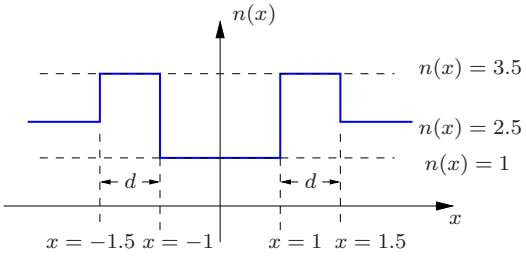

FIG. 4.3. *Sketch of the layout of the air-filled cavity used in the second example.*

the reference solutions are marked with dots. By manual inspection it is possible to confirm that the solutions where both methods are in good agreement are the only physical resonances of the problem in the spectral region. For our solution we used first order finite elements on a grid with a step size of $h = 0.003$. In the exterior we use $L = 25$ Hardy modes and a parameter value $s_0 = 0.87 - 1.14i$.

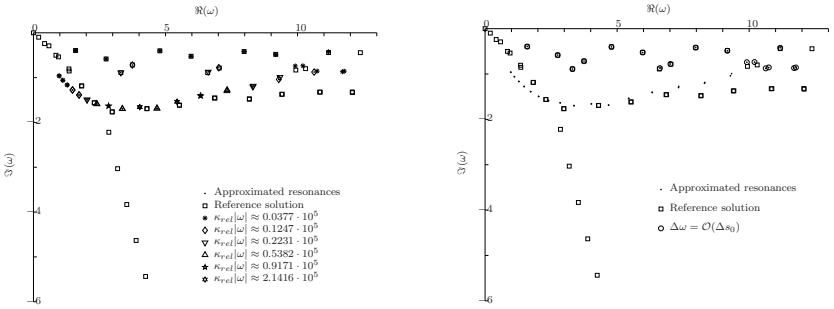

FIG. 4.4. *The spectrum $\sigma(A, B)$ of the second example in the left-hand figure, eigenvalues are marked corresponding to their weighted condition numbers, in the right-hand side figure eigenvalues with $\Delta\omega = \mathcal{O}(\Delta s_0)$ are marked.*

We can see that for this example there exist many spurious solutions with very

low weighted condition numbers, which means that the approach of utilizing condition numbers is not satisfactory for the detection of spurious solutions. However, the right-hand side image of Figure 4.4 shows that again all physical solutions respond to perturbation of s_0 with a perturbation in the order of Δs_0.

Next, we will compute the regions of convergence for these two examples. We set different values for the rate of convergence κ and plot the region in which we can expect a convergence rate of at least κ alongside the spectrum of the problem. These plots for the two one-dimensional examples can be seen in Figure 4.5. It can be seen that for the fist example, even with a convergence rate of $\kappa = 0.85$ no spurious solutions are computed, while for the second example the value is $\kappa = 0.7$. For both convergence rates and our parameter selection we would expect well converged solutions.

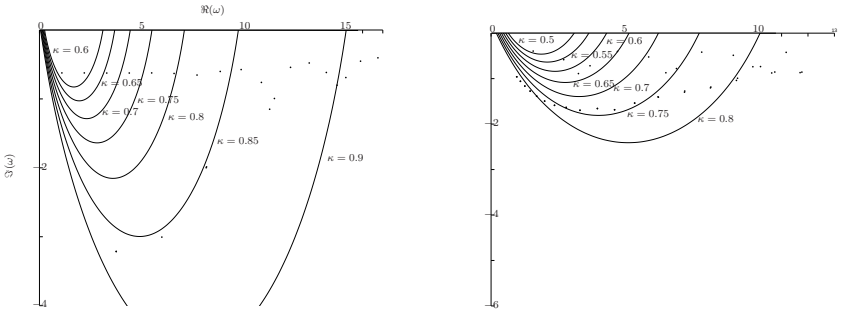

FIG. 4.5. *The eigenvalue spectruma of the first two examples. The left-hand figure shows the convergence monitor for the first example and the right-hand figure shows the convergence monitor for the second example.*

Finally we will give a two-dimensional example with a heterogeneous exterior domain. It is a rectangular air-filled cavity bounded on three sides by a material that is a good conductor. Due to its open side, there is significant radiation into the surrounding air which makes it a good test case for the simulation of open resonators. The mixed grid used for the simulation can be seen in the left-hand plot of Figure 4.6. Moreover, the structure of the spectrum and the position of the spurious solutions combined with their field distributions make a manual identification for of spurious solutions difficult for this example.

The right-hand side plot in Figure 4.6 shows the comparison of the spectrum computed with our MATLAB-code compared with a reference solution obtained with JCMSUITE. We chose $s_0 = 2.05 - 0.6i$ and $L = 10$ as pole condition parameters. The cavity has a witdth of 0.8 and a depth of 0.5, the material within the cavity is air, the second material is a ficitonal material with good electric conductivity that has a permittivity with a high imaginary part to cause damping and a low real part. Some eigenvalues occur in both solutions and can be identified as physical solutions in the spectral region in question, however the identification is not straightforward since some of the spurious solutions have reasonable field distributions. In the right-hand side plot of Figure 4.7, the resonances are marked, whose perturbation is in $\mathcal{O}(\Delta s_0)$ for a perturbation of s_0. We can see that we again correctly identified the spurious solutions for this example. The left-hand side plot of Figure 4.7 shows the computed convergence monitor for the selected parameters. We can see that for a convergence

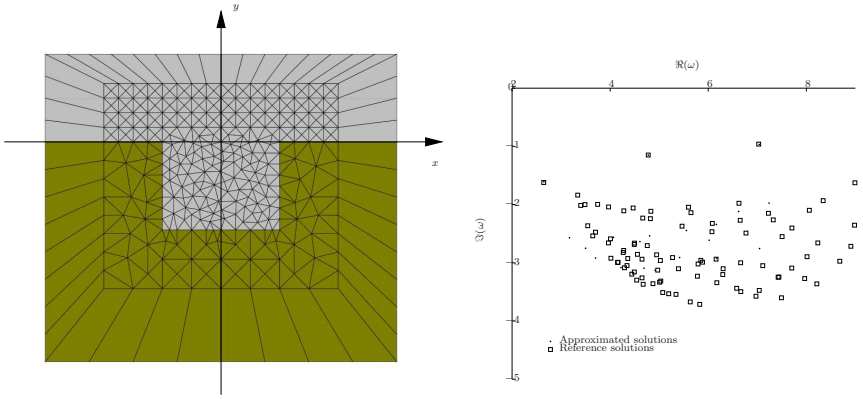

FIG. 4.6. *Left: Mixed grid generated with* JCMgeo *that is used for both pole condition and reference calculations. The interior is discretized with triangles, the exterior with trapezes. Right: Eigenvalue spectrum computed with our method and* JCMsolve *reference solution.*

rate of $\kappa = 0.45$ we can expect the predictions for the first two physical solutions to be correct, for the third physical solution we require a much worse convergence rate and thus also capture some artificial solutions.

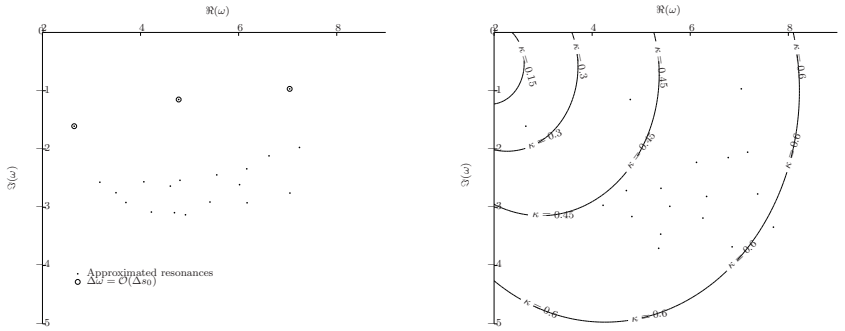

FIG. 4.7. *The spectrum $\sigma(A, B)$ of the third example in the left-hand figure, eigenvalues are marked corresponding to their weighted condition numbers, in the right-hand side figure eigenvalues with $\Delta\omega = \mathcal{O}(\Delta s_0)$ are marked.*

5. Conclusion. We have presented an implementation of the pole condition for Helmholtz resonance problems in one and two space dimensions with possible extension to three-dimensional problems. This implementation has a tuning parameter s_0. We used the dependence of this parameter to detect spurious solutions that are caused by transparent boundary conditions. For this we applied condition numbers which due to their generality yield satisfactory results only for simple model problems. We thus reverted to computing the perturbation of an eigenvalue caused by a perturbation of s_0. This method allowed for a reliable detection of spurious solutions within a resonance spectrum. We complemented it with a convergence monitor for one- and two-dimensional problems in order to obtain a spectral range for which our detection is reliable. Together this yields a practicable framework for the detection of spurious

solutions in the simulation of open resonators without any a priori knowledge of the spectrum or field distribution of the physical solutions.

Acknowledgments. The author would like to acknowledge the funding of this work within project D23 of the DFG research center MATHEON.

REFERENCES

[1] X. Antoine, A. Arnold, C. Besse, M. Ehrhardt, and A. Schädle. A Review of Transparent and Artificial Boundary Conditions Techniques for Linear and Nonlinear Schrödinger Equations. Technical Report 07-34, ZIB, Takustr.7, 14195 Berlin, 2007.

[2] D. Boffi, P. Fernandes, L. Gastaldi, and I. Perugia. Computational Models of Electromagnetic Resonators: Analysis of dge Element Approximation. *SIAM Journal on Numerical Analysis*, 36(4):1264–1290, 1999.

[3] S. Caorsi, P. Fernandes, and M. Raffetto. On the Convergence of Galerkin Finite Element Approximations of Electromagnetic Eigenproblems. *SIAM Journal on Numerical Analysis*, pages 580–607, 2001.

[4] S. Caorsi, P. Fernandes, and M. Raffetto. Spurious-Free Approximations of Electromagnetic Eigenproblems by Means of Nedelec-Type Elements. *ESAIM: Mathematical Modelling and Numerical Analysis*, 35(02):331–354, 2001.

[5] P. Deuflhard and F. Bornemann. *Numerische Mathematik. II: Gewöhnliche Differentialgleichungen*. deGruyter Lehrbuch, 2 edition, 2002.

[6] T. Grossmann, S. Schleede et. al Low-Threshold Conical Microcavity Dye Lasers. *Applied Physics Letters*, 97(6):063304, 2010.

[7] D. J. Higham and N. J. Higham. Structured Backward Error and Condition of Generalized Eigenvalue Problems. *j-SIMAX*, 20(2):493–512, 1998.

[8] T. Hohage. and L. Nannen. Hardy Space Infinite Elements for Scattering and Resonance Problems. *SIAM Journal on Numerical Analysis*, 47(2):972–996, 2009.

[9] T. Hohage, F. Schmidt, and L. Zschiedrich. Solving Time-Harmonic Scattering Problems Based on the Pole Condition I: Theory. *SIAM Journal on Mathematical Analysis*, 35(1):183–210, 2003.

[10] T. Hohage, F. Schmidt, and L. Zschiedrich. Solving Time-Harmonic Scattering Problems Based on the Pole Condition II: Convergence of the PML Method. *SIAM Journal on Mathematical Analysis*, 35:547, 2003.

[11] B. Kettner and F. Schmidt. Meshing of heterogeneous unbounded domains. pages 26–30. Springer-Verlag, October 2008.

[12] L. Nannen. *Hardy-Raum Methoden zur numerischen Lösung von Streu- nd Resonanzproblemen auf unbeschränkten Gebieten*. Phd thesis, 2008.

[13] J. Nédélec. Mixed Finite Elements in $\mathbb{R}^3$. *Numerische Mathematik*, 35(3):315–341, 1980.

[14] L. Nannen and A. Schädle. Hardy Space Infinite Elements for Helmholtz-Type Problems with Unbounded Inhomogeneities. *Wave Motion*, 48(2):116–129, 2011.

[15] J. Pomplun, S. Burger, L. Zschiedrich, and F. Schmidt. Adaptive Finite Element Method for Simulation of Optical Nano Structures. *phys. stat. sol. (b)*, 244:3419 – 3434, 2007.

[16] K. D. Paulsen and D. R. Lynch. Elimination of Vector Parasites in Finite Element Maxwell Solutions. *IEEE Transactions on Microwave Theory and Techniques*, 39(3):395–404, 1991.

[17] D. Ruprecht, A. Schädle, F. Schmidt, and L. Zschiedrich. Transparent Boundary Conditions For Time Dependent Problems. *SIAM J. Sci. Comput.*, 30(5):2358–2385, 2008.

[18] F. Schmidt. An Alternative Derivation of the Exact DtN-Map on a Circle. Technical report, Zuse Institute Berlin, 1998.

[19] F. Schmidt. *Solution of Interior-Exterior Helmholtz-Type Problems Based on the Pole Condition Concept: Theory and Algorithms*. Habilitation thesis, Free University Berlin, 2002.

[20] G. W. Stewart and J. Sun. *Matrix Perturbation Theory*. Academic Press, 1990.

[21] G. W. Stewart. *Matrix Algorithms Volume II: Eigensystems*. Matrix Algorithms. Society for Industrial and Applied Mathematics, 2001.

[22] J. H. Wilkinson. *The Algebraic Eigenvalue Problem*. Monographs on numerical analysis. Clarendon Press, 1988.

[23] L. Zschiedrich, S. Burger, B. Kettner, and F. Schmidt. Advanced Finite Element Method for Nano-Resonators. In M. Osinski, F. Henneberger, and Y. Arakawa, editors, *Physics and Simulation of Optoelectronic Devices XIV*, volume 6115, pages 164 – 174, 2006.